CHAPTER ONE

INTRODUCTION

1.1 Superconductivity and Properties of Superconductors

Superconductivity is the vanishing of electrical resistance of a conductor at very low temperatures. It was discovered by Kamerlingh Onnes in 1911 at Leiden, Holland that pure frozen mercury had its electrical resistance disappear when its temperature was reduced below 4.2Kand a current of order 10^5 Amperes flows. Other metals, alloys and doped semiconductors were found to have this property. The phenomena of superconductivity is manifested in the electrical resistance vanishing at a finite temperature called the critical temperature and denoted by T_c. In his own words, "The experiment left no doubt that as far as the accuracy of the measurement went, the resistance disappeared. At the same time, however, something unexpected occurred. The disappearance did not take place gradually, but abruptly. From $\frac{1}{500}$, the resistance at 4.2K drops to a millionth part. At the lowest temperature, 1.5K, it could be established that the resistance had become less than a thousand – millionth part of that at normal temperature. Thus, the mercury at 4.2K enters a new state, which, owing to its particular electrical properties, can be called the state of superconductivity" (Onnes, 1911).

One may wonder how an experiment can show that the resistance is identically zero. All measuring devices have a limit to their sensitivity, experimental uncertainties are always present and so experimentally it is only possible to establish an upper limit on the observed resistance. This limit, however,

turns out to be exceedingly small. The data shows that the resistivity of a superconductor is below 10^{-27} Ωcm (for comparison

Resistivity of copper which is an excellent conductor is10^{-9} Ωcm). So there is no doubt that we are dealing with ideal conductivity that is total vanishing of electrical resistance.
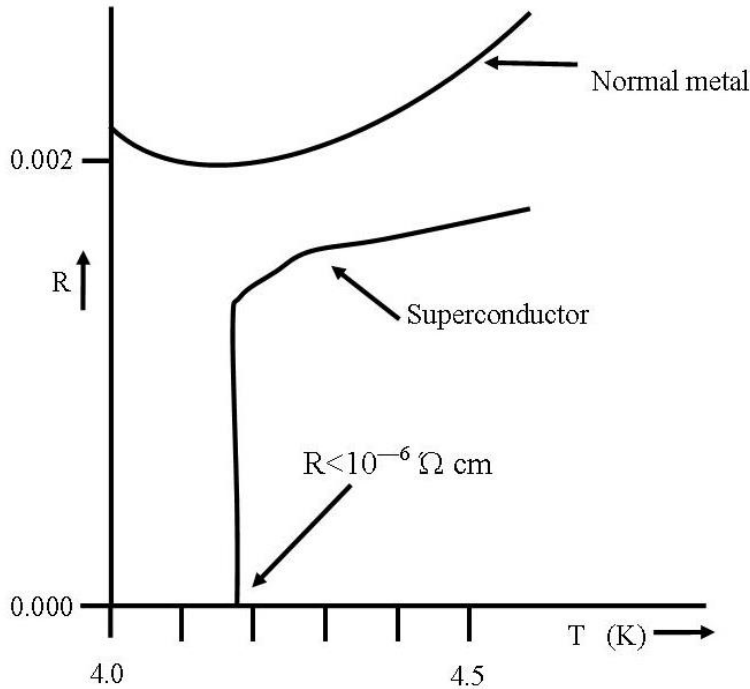

Figure 1.1. Temperature dependence of a normal metal and a superconductor. Kumar (2010)

A metal ring in the superconducting state with induced electric current results into current not being damped and forever circulating around the ring. Collins (1959) showed that even after 2½ years there was no change in the current circulating around such a ring.

Superconductivity exhibited by metals, alloys and doped semiconductors is nowadays called convectional or classical superconductivity (Vladimir, et. al 1990).

In 1933, W Meissner and R. Ochsenfeld discovered that a metal cooled to superconducting state in a moderate magnetic field expels the field from its interior and this is called Meissner Effect (Meissner, et. al, 1933). Magnetic fields do not penetrate into a superconducting sample. At temperature above T_c just as in any normal metal in an external field there will be a finite magnetic field inside the sample. When we start decreasing the temperature without removing the external field we will find that at the moment the superconducting transition occurs, the magnetic field will be expelled from the sample i.e B=0. In all metals, other than ferromagnetic, the magnetic fields created by the elementary atomic currents are oriented chaotically in the metal and cancel out, therefore, B = 0 in the absence of an external field. In presence of an external field, H, there appears finite induction B such that,

$$B = \mu H \tag{1.1}$$

where μ is the permeability, $\mu > 1$ for paramagnetics, $\mu < 1$ for diamagnetics and $\mu = 0$ for superconductors. In superconducting state, a superconductor exhibits perfect diamagnetism. Meissner and Ochsenfeld in 1933 discovered that below the critical temperature $(T < T_c)$, if a superconductor is placed in a magnetic field, the magnetic field is expelled from the interior of a superconductor. Further if H> H_c or T > T_c, the flux penetrates the superconductor, because then the material is non-superconducting and behaves like a normal conductor. The minimum magnetic field necessary to destroy superconductivity is called the critical magnetic field and denoted by H_c. The point noteworthy here is that not only a magnetic field is excluded for $T < T_c$ as the superconductor is placed in a magnetic field, but also a

field present in an originally normal sample is expelled, as shown in Figure 1.2 (a) and (b).
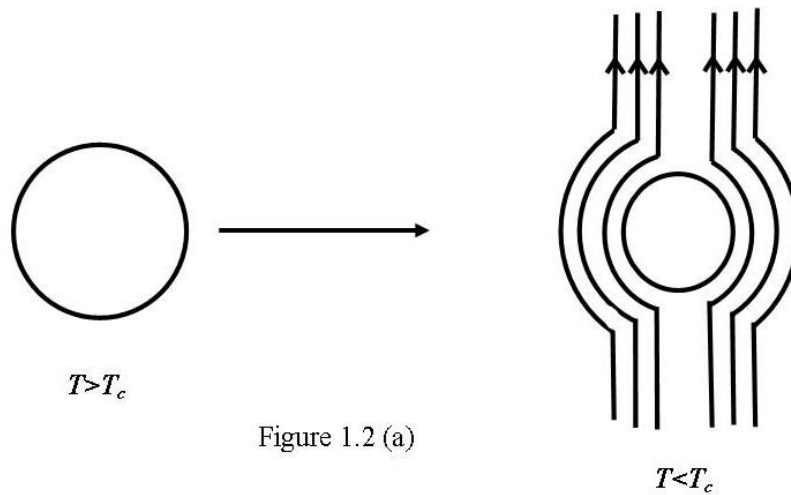

$T>T_c$

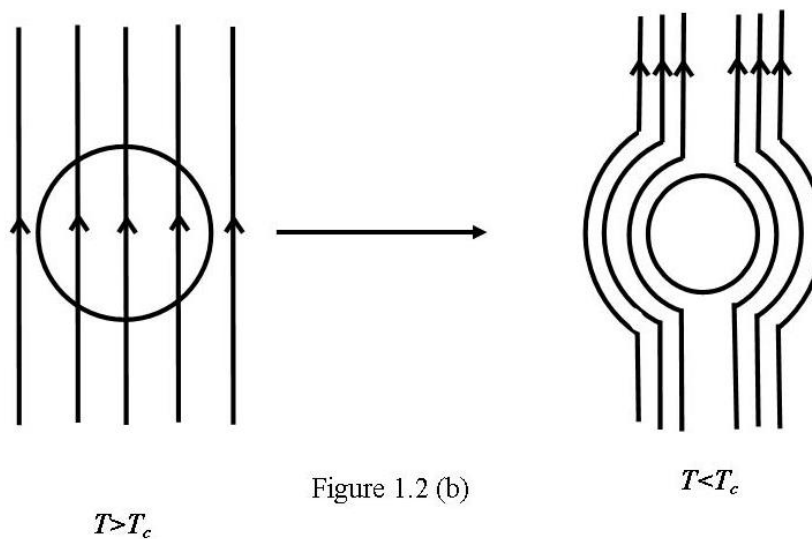Figure 1.2 (a)

$T<T_c$

Figure 1.2 (b)

$T<T_c$

$T>T_c$

Figures 1.2 (a) and (b) show Meissner Effect

1.2 The Cooper pair

In BCS theory it was postulated that in the superconducting state the electrons within a "shell" of width $\sim k_B T_c$ around the Fermi energy tend to form pairs called the Cooper pairs, a sort of giant "dielectronic molecule" whose radius is huge compared

to the average distance between electrons (so that between any two electrons forming a Cooper pair, there are billions of other electrons, forming their own pairs). The creation of Cooper pairs can be understood as follows; an electron tends to create a slight distortion of the elastic lattice as it moves because of the Coulomb attraction between the negatively charged electron and positively charged lattice. If the distortion persists for a brief time, a second electron will feel the distortion and be affected by it. Under certain circumstances, this can give rise to a weak indirect attractive interaction between the two electrons which may more than compensate their Coulomb repulsion. Coulombic repulsive interaction takes place between electrons and its energy is given by V(r) $=(1/4\pi\varepsilon_0)\, e^2/r$, where e is the electrical charge, r is the distance between the electrons, ε_0 is the permittivity in vacuum. It is necessary to overcome the Coulombic interaction to enable the electron pair to be formed. The Coulombic interaction in the medium can be written as,

$$V(r) = (1/4\pi\varepsilon)\, e^2/r = (1/4\pi\varepsilon_0)\, e^2/r - (1/4\pi r)e^2(1/\varepsilon_0 - 1/\varepsilon) \qquad (1.2)$$

where ε is permittivity in the medium. V(r) can be weakened if $\varepsilon_0 < \varepsilon$, which means that an attractive force between electrons in opposition to Coulombic repulsive interaction is generated with the medium. If one electron in the crystal attracts neighboring positive ions, a nearby second electron will be pulled by the positive charges. This means that an attractive interaction throughout the medium is generated between electrons and overcomes the Coulombic interaction locally for a short time, becoming an origin of the formation of Cooper pairs as shown in Figure 1.3.
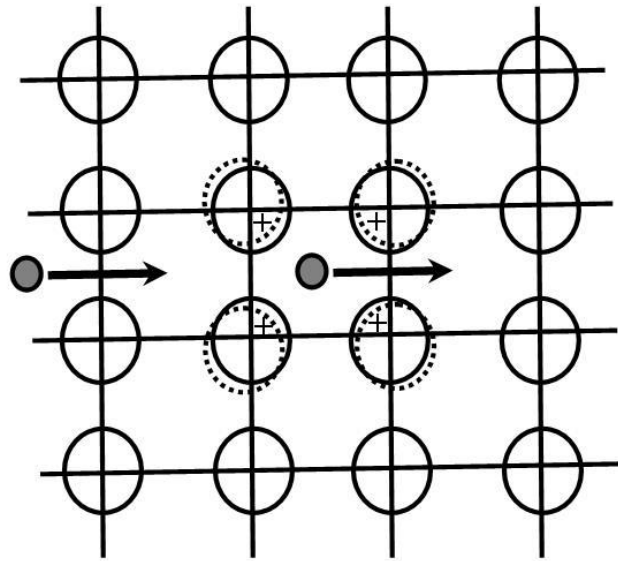
Figure 1.3. The generation of attractive force between electrons in the crystal. The second electron moving in the crystal is attracted by the positive charge of the crystal ions which is produced by Coulomb interaction with the first electron passing there. Thus, two electrons interact with each other through the medium. Bhattacharya (2011)

Two electrons can bind together in the momentum space but not real space to form bound pairs. The two electrons in a Cooper pair have opposite momenta and spins.

This is the mechanism via electron-phonon interaction, and it explains the origin of conventional low-T_c superconductors (Frolich, 1950). It also confirms that Cooper pairs are formed in high-T_c superconductors. However, the mechanism of the attractive force of a Cooper pair has not yet been established and is still being investigated. The interaction of two electrons via phonons can be visualized as the emission of a "virtual" phonon by one electron, and its absorption by the other, as shown figure 1.4.
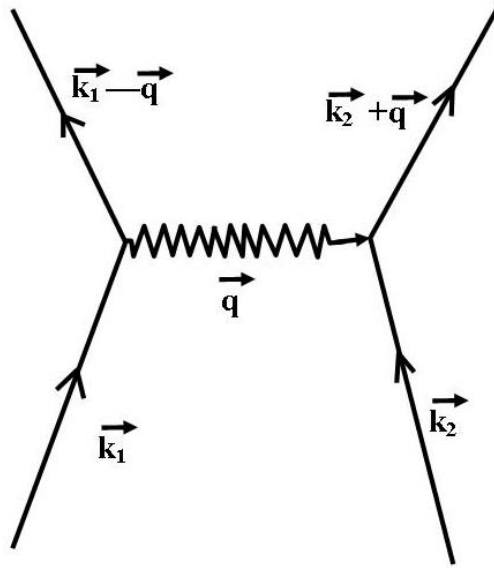
Fig.1.4. Illustration of electron-electron interaction via exchange of a virtual phonon of momentum of $\overrightarrow{hq}$. Mourachkine (2002)

An electron in state $\overrightarrow{k_1}$ emits a phonon, and is scattered in state $\overrightarrow{k_1}$-$\vec{q}$. The electron in the state $\overrightarrow{k_2}$ absorbs a phonon with momentum q and leads to state$\overrightarrow{k_2}$+$\vec{q}$. Figure 1.4shows the direct way of calculating the force which attracts the two electrons. However, it is necessary to know the spectrum of the lattice vibrations in a solid because, in different solids, phonons propagate at different frequencies (energies) (Mourachkine, 2002).

1.2.1 The size of an electron pair

The spatial spread $\xi$of electrons in a Cooper pair is (using uncertainty relation) given by equation,

$$\xi = \frac{\hbar v_F}{k_B T_c},$$
(1.3)

Where$v_F$is Fermi velocity and $\xi$is the distance between two electrons in a Cooper pair, also known as the *Pippard coherence length* or the *BCS coherence length*,

(Pippard, 1953). For example, BCS coherence length,$\xi \approx 10^{-6}$m,is roughly obtained assuming the typical Fermi velocity$v_F \approx 10^6$ m/s whenT_c <25K.

The size of a Cooper pair, $\xi \cong 10^{-4}$cm which is 10^4 times the lattice spacing or period of crystal lattice (the distance between the electrons, a $\cong 10^{-8}$cm). Thus $\xi \gg$ a.

1.3 Field-Dependence properties of High-Temperature Superconductors

1.3.1 Anisotropy and Superconductivity.

A superconducting state is defined by transition temperature T_c, at which materials exhibits zero resistance on cooling. Apart from the transition temperature, other properties characterizing the high-T_c superconductors are critical magnetic field, penetration depth, coherence length, critical current density and weak link, energy gap and so forth. In this thesis field-dependent properties of HTSC are investigated these are critical magnetic field, penetration depth, coherence length and energy gap. The crystal structure of high-T_c superconductors is highly anisotropic. This feature has important implications for both physical and mechanical properties of HTSC. In high-T_c superconductors, electrical current is carried by holes induced in the oxygen sites of the CuO_2 sheets. The electrical conduction is highly anisotropic, with a much higher conductivity parallel to the CuO_2 plane than in the perpendicular direction. Other superconductivity properties such as coherence length (ξ), penetration depth (λ), and energy gap (Δ) are also anisotropic. The mechanical properties of high-T_c superconducting materials are also very anisotropic. For example, in YBCO, upon cooling, the lattice contracts far more along a–b planes than along c axis. Torque

magnetometry measurements have been made for several high-T_c superconductorsfor studying anisotropy (Kogan, 1988 and Farrell et al., 1990). The relation between the effective mass ratio and the anisotropic parameter γ_a, the coherence length ξ, the upper critical field H_{c2}, and the penetration depth $\lambda$are given by the relations,

$$(m_c/m_{ab})^{1/2} = \gamma_a = \xi_{ab}/\xi_c = H_{c2//}/H_{c2\perp} = \lambda_c/\lambda_{ab} \qquad (1.4)$$

where// denotes the case where magnetic field is applied parallel to the layer and $\perp$ corresponds to the perpendicular case. Using the angle θ between the direction parallel to the CuO$_2$ layer and the direction of magnetic field, we have,

$$H_{c2}(\theta) = H_{c2//}/(\cos^2\theta + \gamma_a^2 \sin^2\theta)^{1/2} \qquad (1.5)$$

 This anisotropic model is called the effective mass model (Blatter et al., 1992). For Tl2212, anisotropy of $\sim 10^5$ is found for the ratio of the mass along the c axis to that of a–b plane. A similar large ratio is obtained for Bi2212 compound. In Y123, the value of the ratio is found to be ~ 25, which is much smaller compared to Bi and Tl compounds. The anisotropy factor of high-T_c superconductor at the optimally doped composition is related to interlayer spacing between CuO$_2$ layers in the unit cell. It has also been noted that increasing carrier doping or substituting ions on the blocking layer for certain other ions such as Pb in Bi2212 reduces anisotropy without changing the interlayer spacing significantly.

The wave function of Cooper pairs is confined in the CuO$_2$ layer and two dimensional properties become remarkable. In this case the Lawrence-Doniach model (Lawrence et al, 1971) is used to explain the anisotropic properties.

By applying the magnetic field to the high-T_c cuprate superconductor, some peculiar features are observed. For instance, (i) because the coherence length is very

short, the cores of the quantized vortices are small so that the pinning strength is weak; (ii) when the vortices vertically penetrate the CuO_2 layers, the vortices bend easily because the superconducting coupling between the CuO_2 layers is weak (Clem, 1991); (iii) the Abrikosov lattice easily melts in the neighbourhood of T_c by the effect of thermal energy (Houghton et al., 1989). As a result, the influence of the thermal fluctuation becomes remarkable in the cuprate superconductors, and the phase transition between the normal conducting state and the superconducting state becomes indistinct.

1.3.2 Magnetic Field and Superconductivity

Magnetic properties of superconductors are as old as the phenomenon of superconductivity discovered by Onnes in 1911 (Onnes, 1911). He found that dc resistivity of mercury suddenly drops to zero at 4.2K. A year later, he discovered that a sufficiently strong magnetic field restores the resistivity in the sample as does a sufficiently strong electric current.

In 1933, Meissner and Ochsenfeld discovered one of the most fundamental properties of superconductors: perfect diamagnetism (Meissner et al, 1933). They found that the magnetic flux is expelled from the interior of the sample that is cooled below the critical temperature in weak external fields. They postulated that below the critical temperature (T $<T_c$), if a superconductor is placed in a magnetic field, the magnetic field is expelled from the interior of a superconductor. This phenomenon is known as Meissner effect. Further, if H $>H_c$ or (T $>T_c$), the flux penetrates the superconductor, because the material is non-superconducting and behaves like a

normal conductor. The magnetic field at which superconductivity is destroyed and the resistivity is restored (normal state system) is called the critical magnetic field and is denoted by H_c. Based on the Meissner effect, the superconducting materials are classified type-I and type-II superconductors. If there is a sharp transition from the superconducting state to the normal state, then this type of material is called a type-I superconductor. This kind of behaviour is shown, in general, by pure metals. In type-II superconductors, there are two values of the critical field: the lower critical field, H_{c_1}, and the upper critical field H_{c_2}. For H $<H_{c_1}$, the field is completely expelled from the superconductor. However, for H $>H_{c_1}$, the magnetic field penetrates the material slowly and continues up to H_{c_2}, beyond which the materials transforms completely from the superconducting state to the normal state. The state below H_{c_1} is called the Meissner state. The state between H_{c_1} and H_{c_2} is called the vortex or mixed state as shown in Figures 1.5 (a) and (b).
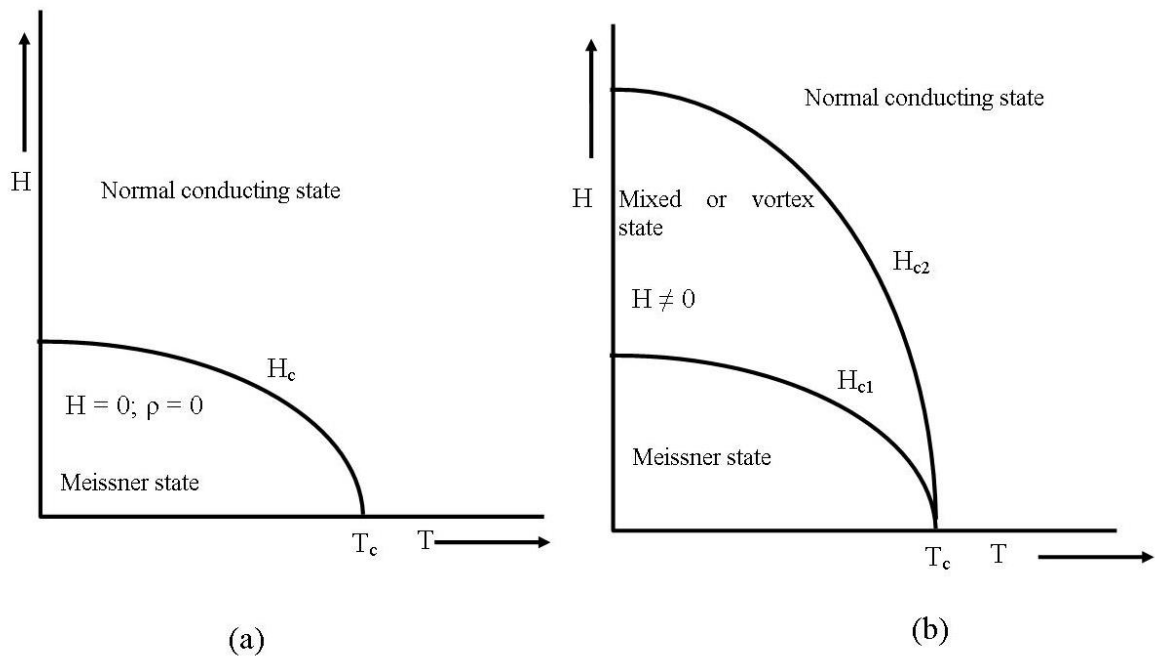

(a)

(b)

Figure 1.5. (a) A type-I superconductor and (b) a type-II superconductor. The Meissner state, mixed state and the normal conducting state separated by the lines H_c, H_{c1} and H_{c2} lines. Bhattacharya (2011)

As schematically shown in figures 1.5 (a), the variation of magnetic field H_c with temperature T for a type-I superconductor is approximately parabolic as given by the equation,

$$H_c(T) = H_c(0)[1 - (T/T_c)^2] \tag{1.6}$$

At fields just above H_{c1}, however, flux begins to penetrate the superconductor in microscopic filaments called vortices which form a regular (hexagonal) lattice. Each vortice consists of a normal core in which the magnetic field is large, surrounded by a superconducting region, and can be approximated by a long cylinder with its axis parallel to the external magnetic field inside the cylinder. The radius of the cylinder is of the order of the coherence length ξ. The super current circulates around the vortex within an area of radius $\sim\lambda$, the penetration depth. The vortex state of a superconductor, discovered experimentally by Shubnikov (1936) and theoretically explained by Abrikosov (1957), is known as mixed state.
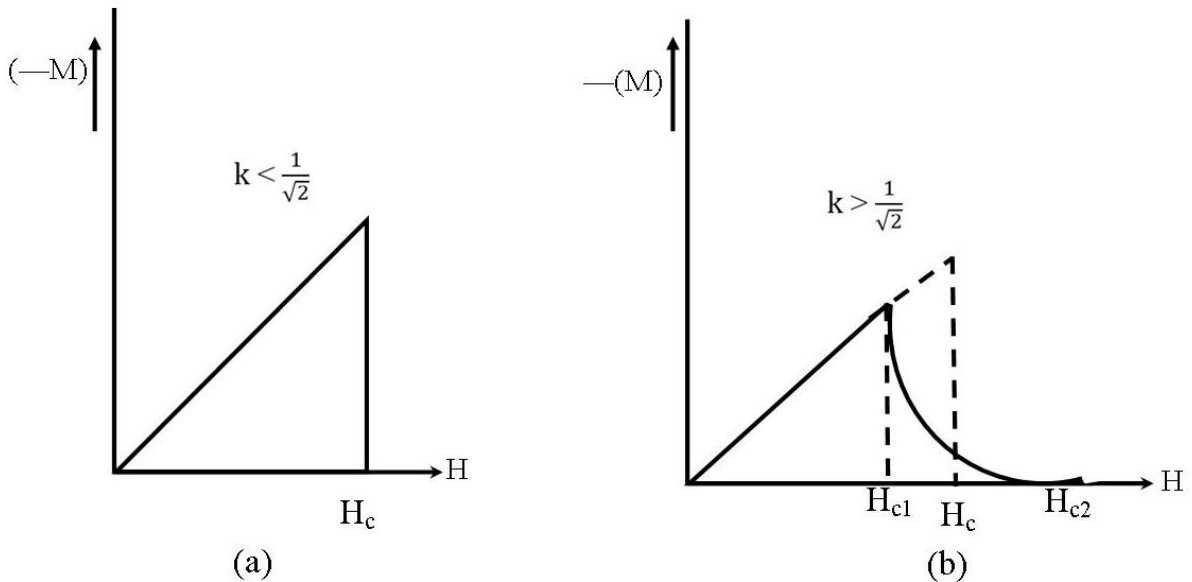
Figures 1.6. Magnetization versus applied magnetic field for (a) type-I and (b) type-II Superconductors. Kumar (2010).

Type-I superconductors show complete Meissner effect, the magnetization (M) versus applied magnetic field as shown in Figures 1.6.

The magnetization drops suddenly at the critical field H $= H_c$. In type-II superconductors, magnetization drops earlier, before reaching the critical field H $= H_c$. There starts penetration of flux in the specimen at a field value of H_{c1} which is lower than H_c. The phase change at H_c represents a first-order phase transition. The transitions at H_{c1} and H_{c2} are of second-order phase transition. The free energies are related as by $F_n > F_s$ where F_n is free energy for normal state and F_s is free energy for superconducting state.

Flux enters at H $> H_{c1}$ and according to Abrikosov, it does so in the form of flux vortices, which assume a triangular lattice structure to minimize their interaction energy. For $H_{c1} <$ H $< H_{c2}$, we have this intermediate phase or Shubnikov phase. At H_{c1}, the first vortex is nucleated and with increasing field, their equilibrium separation is reduced, such that at H_{c2} the normal cores overlap and then, bulk of the material turns normal Figure 1.7.
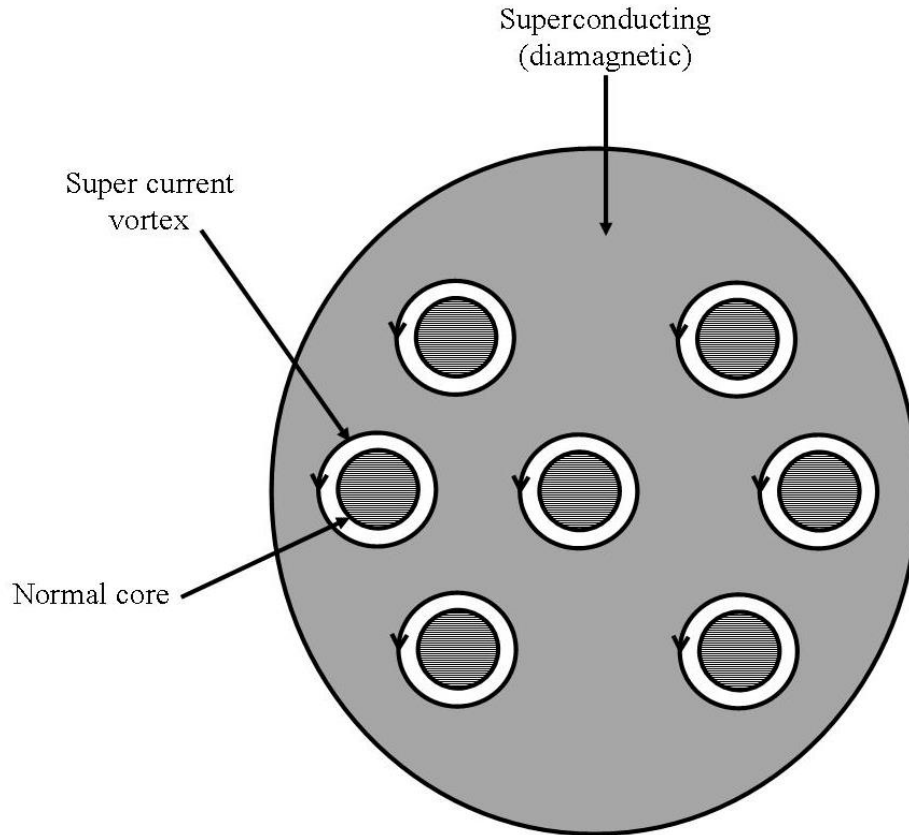
Fig. 1.7. The triangular lattice of vortices in the mixed state. Kumar (2010)

A vortex consists of normal core (a cylinder of normal region parallel to the applied magnetic field) carrying a flux quantum $\phi_0 = 2.07$ x 10^{-15} Webers and diameter 2ξ. This microscopic normal region is surrounded by circulating super-electrons.

A flux vortex is also known as a fluxoid. In the space between the vortices, material remains superconducting; this is where the electric current flows, so the electrical resistance is still absent.

With the application of the field H $>H_{c1}$, normal cores are nucleated, each carrying a quantum of flux ϕ_0. A core is surrounded by a circulating current (of super-electrons), whose super-fluid velocity is quantized and its value given by,

$$v_{s0} = \frac{h}{2m\xi}. \tag{1.7}$$

The super-electrons revolve around the vortex axis like current in a superconducting ring. The closer the super-electrons to the vortex-axis, the faster they circulate. At a shorter distance from the axis, the speed exceeds the critical value v_{s0} and superconductivity is destroyed (inside normal core).

1.3.3 Flux Quantization

In superconductors the magnetic flux (Φ) trapped in a closed superconducting ring is always an integral multiple of a flux quantum Φ_0 given by,

$$\Phi = n\Phi_0 \qquad\qquad\qquad (1.8)$$

Where n is an integer and $\Phi_0 = h/2e = 2 \times 10^{-7}$ G/cm^2, h is Planck's constant and e is the electronic charge; the factors of 2 in the denominator shows that the superconducting ground state is composed of paired electrons. Gough and coworkers (Gough et al., 1987), performed an experiment to measure the flux through a sintered YBCO ring using a weakly coupled superconducting quantum interference device (SQUID) magnetometer. A small source of noise was applied to induce flux jumps. The nature of the flux passing in and out of the ring was clearly observed in the experiment. Gammel et al. in 1987 through the magnetic decoration technique in another experiment while studying flux line arrangement in YBCO single crystals obtained similar results as Gough et al. (Gammel et al., 1987). This observation of flux quantization in high-T_c superconductor clearly indicates that the paired electrons are responsible for the superconducting state.

1.3.4 Coherence Length and Penetration Depth

The "distance" between the two electrons of a Cooper pair is called the coherence length, ξ. In the framework of BCS theory, the intrinsic coherence length, ξ_0 (size of a Cooper pair), is related to the energy gap at T = 0K such that,

$$\xi_0 = \hbar v_F / \pi \Delta(0) \tag{1.9}$$

where v_F is the Fermi velocity (on the Fermi surface) and Δ is the energy gap. The intrinsic coherence length ξ_0 is temperature-independent. And the coherence length ξ is given as,

$$\xi = h v_F / 2\pi^2 k_B T_c \tag{1.10}$$

where k_B is the Boltzmann's constant and Eq. (1.10) shows that the higher the values of T_c in copper oxide superconductors the lower the value of ξ.

In the framework of Ginzburg-Landau theory, the temperature-dependent coherence length, ξ and the intrinsic coherence length ξ_0 are given by the relation,

$$1/\xi = 1/\xi_0 + 1/l \tag{1.11}$$

Where the mean free path of an electron. In most unconventional superconductors i.e. cuprates, the value of ξ is a few periods of the crystal lattice, $\xi_c \approx$ 1-3Å and $\xi_{ab} \approx$ 10-30Å. (Uchida, 1997). In conventional low-T_c superconductors, the coherence length is 1000-1600Å. Which is several orders of magnitude larger than that in high-T_c superconductors. The low value of coherence length means that the coherence volume contains only a few Cooper pairs, implying that the fluctuations may be much larger in the high-T_c superconductors than in conventional superconductors. The low values of coherence length make these materials very sensitive to the presence of local defects such as oxygen vacancies, dislocations, and deviation from the stoichiometry.

BelowH_{c1}, the external magnetic field is excluded from the bulk of a superconducting material by a persistent super current in the surface region, which induces a field that exactly matches the applied field but in the opposite direction. The depth of this surface region is called penetration depth, λ, and the external field penetrates the superconductor in an exponentially decreasing manner. Penetration depth is distance over which an applied magnetic field decays to $1/e$ of its value at the surface. For an isotropic superconductor, the lower critical field H_{c1} is related to the penetration depth such that,

$$H_{c1} \approx \Phi_0/\lambda^2 \qquad (1.12)$$

Where Φ_0 is the flux quantum. The value of the penetration depth can be obtained from the magnetization of thin superconducting crystal, muon spin rotation, kinetic inductance or microwave measurements. Anisotropy in penetration depth can be estimated from flux decoration and magnetic torque experiments. For YBCO single crystal, the value of $\lambda_{ab}(T \rightarrow 0)$ is obtained as 1400 Å (Krusin-Elbaum et al, 1989). The two-fluid model describes the temperature dependence of penetration depth such that,

$$\lambda(T) = \lambda(0) \left[1 - (T/T_c)^4\right]^{\frac{-1}{2}} \qquad (1.13)$$

For weak coupling BCS superconductor, the $\Delta\lambda = [\lambda(T) - \lambda(0)]$ varies exponentially with temperature (Muhlschlegel, 1959). If there are nodes in the energy gap, then $\lambda(T)$ varies linearly with T (Hardy et al, 1993).

The magnitude of the penetration depth depends on the material and temperature, and decreases exponentially towards the core as shown in Figure 1.8.
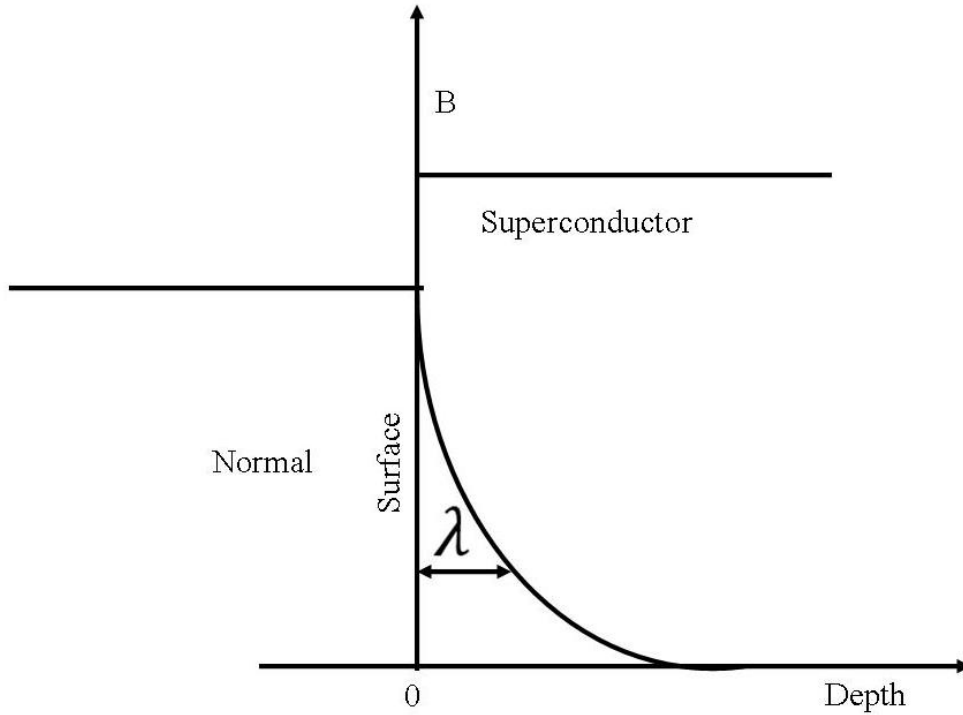
Fig. 1.8. The penetration of the magnetic field into the superconducting sample. Mourachkine (2002)

The magnitude of the penetration depth is directly related to the super fluid density n_s, i.e.,

$$\lambda^2(T) = m^* c^2 / 4\pi e^2 n_s(T) \qquad (1.14)$$

Where m^* is the effective mass of charge carriers, e is the electronic charge and c the speed of light in vacuum.

Both the penetration depth, $\lambda(T)$ and the coherence length $\xi(T)$ are temperature dependent quantities. The ratio $\kappa = \lambda(T)/\xi(T)$ is called the Ginzburg-Landau (GL) parameter and is an important factor by which the magnetic properties of a superconductor are decided. For $\kappa \ll 1$ (i.e. $\lambda \ll \xi$), we have type-I superconductors and superconductors having $\kappa \gg 1$ (i.e. $\lambda \gg \xi$) are type-II superconductors.

1.4 The Energy Gap

In Landau's concept of the Fermi liquid, excitations, called quasiparticles, are bare electrons dressed by the medium in which they move. Quasiparticles can be created out of the superconducting ground state by breaking up pairs, but only at the expense of a minimum energy of Δ per excitation. This minimum energy, Δ, is called the energy gap. The BCS theory predicts that, at T = 0K, Δ is related to the critical temperature by $\Delta = 1.76\ k_B T_c$ for any superconductor. This turns out to be nearly true, and where deviations occur they can be understood in terms of modifications of the BCS theory. The manifestation of the energy gap in tunneling provided strong confirmation of the theory.

The energy gap in a superconductor is quite different in its origin from that in a semiconductor. From the Band theory, energy bands are as a consequence of static lattice structure. In a superconductor, the energy gap is far smaller, and results from an attractive force between electrons in the lattice which plays only an indirect role. In conventional superconductors, the energy gap arises only at temperatures below T_c, and varies with temperature. The gap occurs on either side of the Fermi level as shown in figure 1.9.

The density of states near the Fermi level E_F in a superconductor, showing energy gap 2Δ at T = 0 and in a normal metal, all the states above the gaps are assumed empty and those below occupied.
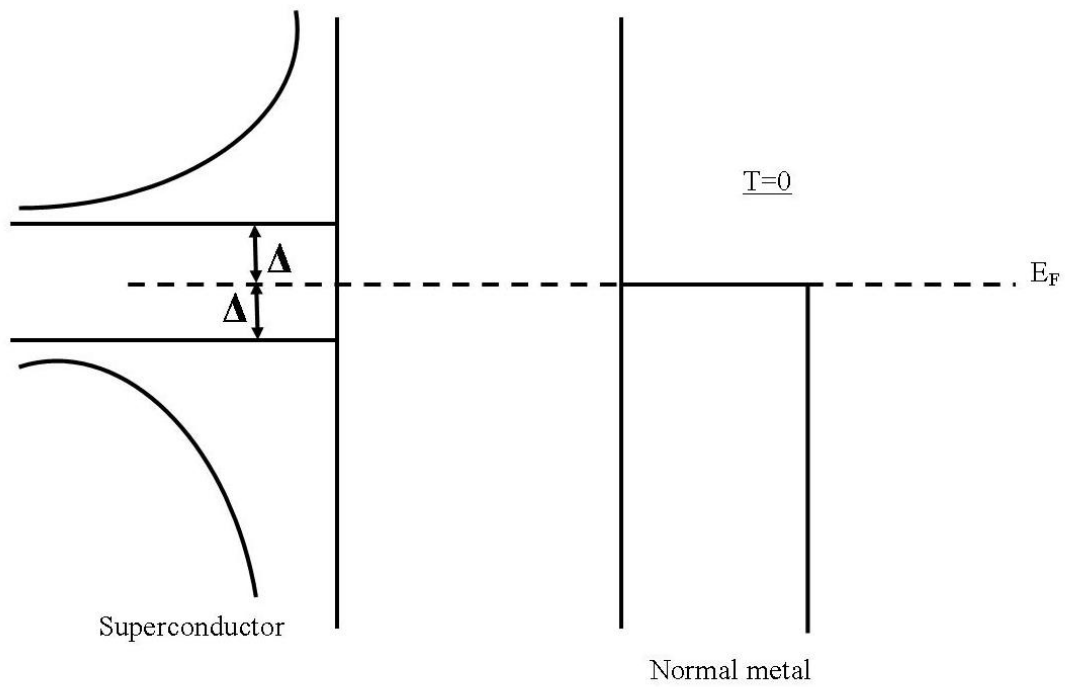
Fig. 1.9. The density of states near the Fermi level in a superconductor showing the energy gap of 2Δ at T=0 and in a normal metal. Mourachkine (2002).

The energy gap is a function of temperature and the temperature dependence is as shown in Figure 1.10.
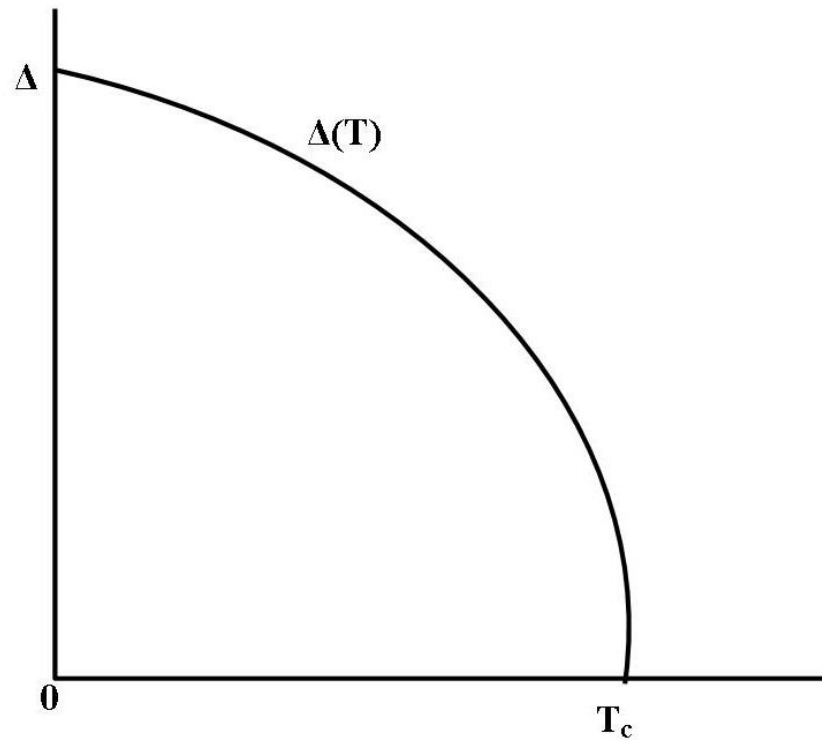
Δ

$\Delta(T)$

0

T_c

c.

Fig. 1.10. Showing the energy gap dependence on temperature. Kumar (2010)

For a weakly coupled BCS superconductor, the energy gap Δ at 0K is related to T_c and is given by (Andreev, 1964, Khanna, 2008).

$$2\Delta(T)/k_B T_c = 3.52 \tag{1.15}$$

For high T_c superconductors, a higher value of the ratio of energy gap–to–T_c is observed as compared to the weakly coupled BCS superconductor. Anisotropy in the gap value along the c axis and in the ab plane is also noticed. For YBCO, the energy gap–to–T_c ratio $[2\Delta(0)/k_B T_c]$ has been found to be 3.5 for tunneling perpendicular to the Cu–O plane and value of ~ 6 has been found for tunneling in Cu–O plane (Tsai et al, 1989). A similar higher value of the same ratio is also observed for tunneling in the Cu–O plane in Bi–Sr–Ca–Cu–O (Boekholt et al, 1991, Ozyuzer et al, 2000 and Huang et al, 1989), Tl–Ba–Ca–Cu–O (Ozyuzer et al, 1999 and Takechi et al, 1989) and   Hg–Ba–Ca–Cu–O (Jeong et al, 1994). Tom Timusk and Bryan Statt in an

experimental survey found out that the value of the energy gap of most of HTSC lies between 10meV and 100meV (Timusk et al, 1999).

Table 1.1 Shows values of the ratio of the energy gap–to–T_c for some high T_c superconductors.

High T_c Superconductors	T_c (K)	Δ(meV)	$2\Delta/k_B T_c$	Reference
$YBa_2Cu_3O_{7-\delta}$	85	20	6	J.S. Tsai, et al., 1989
$Bi_2Sr_2CaCu_2O_{8+\delta}$	62	20	7.5	L. Ozyuzer et al., 2000
$Bi_{1.7}Pb_{0.3}Sr_2CaCu_2O_x$	96	34	6.3	Q. Huang et al., 1989
$Tl_2Ba_2Cu_3O_x$	86	25	6.7	L. Ozyuzer et al., 1999
$Tl_2Ba_2Ca_2Cu_3O_x$	114	30	6.1	I. Takechi et al., 1989
$HgBa_2Ca_2Cu_3O_{8+\delta}$	132	48	8.0	G. T. Jeong et al., 1994

For high T_c superconductors the ratio of energy gap–to–T_c is given by Eq. (1.16) (Vedeneev, 1994, Khanna, 2008).

$$2\Delta(T)/k_B T_c = 5 - 8 \tag{1.16}$$

In high temperature superconductors, because of the layered structure, the carrier motion is quasi-two-dimensional, which favors better pairing. Therefore, even carriers far from E_F bind, leading to a large value of Δ. The high value of the ratio $\Delta(0)/E_F$ indicates that the fraction of carriers paired is much larger in HTSCs than in conventional superconductors.

1.5   Statement of the Problem

Regardless of the differences between the properties of the BCS type and HTSC superconductors, the pairing of electrons to form what are called Cooper pairs is common among the two types of superconductors. However, in the BCS type superconductors, it is the electron-phonon interaction that leads to the formation of

Cooper pairs, whereas the mechanism of electron-electron pairing in HTSC is still not exactly known.

In HTSC, charge carriers are known to travel along the Cu-O planes. It is also surmised that there could exist dipoles since electrons and positive ions of equal and opposite charge do exist. If these dipoles interact with the electrons constituting the electron-electron (Cooper pair) pair, and the Cooper pairs oscillate, this leads to the creation of an electric field E along the Cu-O planes. This informs the need to study the effect of such an electric field on the energy gap Δ, and consequently; the superconducting order parameter.

Wherever there exist electric currents and electric fields, there will exist magnetic fields. To study the effect of magnetic fields, it is necessary to apply external magnetic field and study its effect on electron-electron pairing and also the transition temperature.

It is hoped that such studies could lead to a better understanding of the mechanism of electron-electron interaction in HTSC, and then it could lead to proper understanding of the HTSC properties.

1.6 Objectives of the Study

1.6.1 General Objective of the Study

To study the effects of the fields on the thermodynamic properties of HTSC Cuprates.

1.6.2   Specific Objectives of the Study

1) To determine the value of energy gap (Δ) of a YBCO system due to effect of an electric field E caused by oscillating Cooper Pairs along CuO planes.

2) To determine the effect of Δ (energy gap) on transition temperature (T_c) of aYBCO system.

3) To investigate the effect of applied magnetic field H on lattice constant a and α (the ratio of the time taken by an electron to move through the lattice constant a to the time taken to move once on a circular path).

4) To determine the value of the transition temperature at which BSCCO and YBCO systems change from superconducting (mixed/vortex) state to normal state under influence of an applied external magnetic field.

5) To investigate the effect of applied magnetic flux per plaquette on transition temperature T_c of some high temperature superconductors.

1.7   Significance of the Research.

The main goal of all research in the field of high temperature superconductivity is to be able to understand the electron-electron pairing mechanism, and to increase the values of T_c further towards room temperature. Before and after the formulation of the BCS theory in 1957, there has been a remarkable relationship between superconductivity and magnetic fields. Continual research into the field dependence of the properties of high temperature superconductors may unveil the mystery of the pairing mechanism in high T_c superconductors.

1.8 Justification of the Study.

Conventional superconductivity is the consequence of phonon-mediated attraction between two electrons resulting in the formation of Cooper pairs. High-temperature superconductivity cannot be explained by the normal BCS theory. High-temperature compounds are in general poor conductors but exhibit superconductivity at comparatively higher temperatures. Thus other interactions have to be explored to explain superconducting properties of such materials. These poor conductors have one or more CuO_2 planes separated by insulating oxide layers. It is believed that superconductivity takes place along the CuO_2 planes. Therefore, electron-electron pairing interaction under the application of uniform magnetic field on a two-dimensional square lattice of a superconductor crystal is to be investigated. The effect of oscillating Cooper pairs on the energy gap due to electric field E along the CuO_2 planes has to be investigated. The effect of effective magnetic flux on the transition temperature of high T_c superconductors has also to be investigated.

The effect of magnetic field on a superconducting state is as old as the field of superconductivity itself because a year later after the discovery of superconductivity, K. M. Onnes discovered that a sufficiently strong magnetic field restores the resistivity in the sample as does sufficiently strong electric current. It was later discovered by W. Meissner and R. Ochsenfeld that superconductors show perfect diamagnetism. They found out that the magnetic flux is expelled from the interior of the sample that is cooled below T_c in weak external magnetic fields (Meissner, et al. 1933). They also showed that when a metal ring with current circulating around it and a superconducting sphere is placed above it and the temperature lowered below T_c,

the sphere will be suspended above the ring (Levitation). This idea and its application in magnetic levitated trains was discovered before the BCS theory was formulated.

Later Shubnikov and co-workers found the unusual behaviour of superconductors in external magnetic fields. They discovered existence of two critical magnetic fields in a state known as mixed state or Shubnikov phase (Shubnikov, et al. 1937). Shubnikov's experiments were later explained theoretically by Abrikosov (Abrikosov, 1957).

The energy gap is one of the important features of superconductivity. Angle-resolved photoelectron spectroscopy in Bi2212 has been used to investigate the energy gap in different k directions. And an anisotropy of the gap value in ab plane was noted (Shen et al, 1993). Low-temperature scanning tunneling microscopy in Hg1201 shows the presence of different gaps to different crystallographic faces, implying a non-BCS electron-electron pairing mechanism (Jess, et al. 1996).

CHAPTER TWO

LITERATURE REVIEW

2.1   Classification of superconductors

Superconductors can be classified using the following criteria

i)   Physical properties-type I (for phase transition of first order) or type II (phase transition is second order)

ii)   Theory for explaining – conventional or classical (explained by BCS theory and its derivatives) and unconventional if not explained by BCS theory (Bardeen J, 1957).

iii)   The temperature-high temperature superconductors that exhibit superconductivity at temperatures above 30K.

iv)   The chemical elements i.e. mercury and lead, alloys (niobium-titanium, germanium-niobium) or ceramics (YBCO, magnesium diboride) or organic compounds (fullerenes, carbon nanotubes).

The number of superconducting materials is slowly approaching tens of thousands. They can be classified into several groups according to their properties:

- Metals or elements
- Binary alloys and compounds
- Intermetallic compounds (A15 materials)
- Chevrel phases
- Semiconductors
- Organic Quasi-One-dimensional superconductors

- Heavy fermions

- Oxides

- High T_c superconductors (copper oxides)

- Dopped semiconductors, etc.

The current state of typical superconducting materials is described below.

2.1.1 Elements

After the discovery of the superconductivity of mercury (Hg) in 1911, it was confirmed that Pb and Sn also become superconductors, and afterwards the superconducting elements were identified one by one. More than 30 elements become superconducting on cooling to an extremely low temperature. In addition it was confirmed that over 20 other elements become superconducting at high pressure. About half of the elements in the periodic table are currently known to be potential superconductors, but the superconductivity of alkali metals such as Na, magnetic materials such as Co and Ni, and low resistivity materials such as Au, Cu and Ag has not been confirmed yet.(Poole, et. al. 1995, Buckel, et al. 2004).

The superconductors of practical use are Nb and Pb, whose T_c values are higher than the temperature of liquid Helium (4.2K). The crystal structure of Nb is body-centered cubic (bcc) and its T_c is 9.25K. Nb is a type II superconductor and its B_{c2} is about 0.3T. B_{c2} is related to the resistivity ρ, (Kim., et al. 1965). Such that,

$$B_{c2} = \mu_0 H_{c2} = 3.1 \times 10^3 \mu_0 \rho \sigma T_c \tag{2.1}$$

Where σ is an electronic specific heat coefficient. A small amount of oxygen or nitrogen as an impurity in Nb increases $\mu_0 H_{c2}$ because ρ increases. T_c similarly

changes because of impurities. The introduction of oxygen or nitrogen atoms into the crystal lattice usually decreases T_c. This is because of the fact that electron density of the state changes at the Fermi surface due to the existence of the impurity atoms. The crystal structure of Pb on the other hand, is face-centered cubic (fcc), and its T_c is changed by the introduction of minute amounts of doping impurities. For instance, the doping of Hg or Tl reduces T_c considerably, whereas the doping of Bi, As or Sn raises T_c by about 1K. Although Pb is originally a type I superconductor, it becomes a type II superconductor because of the increase in ρ when small amounts of doping impurities are introduced.

2.1.2 Alloys

The number of superconducting alloys exceeds one thousand. The crystal structure and physical properties of the principal metallic ingredient are reproduced in the alloy and change continuously as the percentage of the additional element is increased, but the superconducting characteristics can be much superior to those of the unalloyed metals. Nb–Ti alloy is commercially used for many applications and is one of the most important superconducting materials. According to the BCS weak coupling theory, the T_c is given by

$$T_c = 1.13\theta_D e^{\frac{-1}{N(E_F)V}} \tag{2.2}$$

where θ_D is the Debye temperature, $N(E_F)$ is the density state of the electron on the Fermi surface and V is an interaction between electrons. The maximum value of T_c reaches in the vicinity of 50% by weight of Ti (Collings, 1986).

2.1.3 A15 Type Compound

A15 compounds were discovered by Hardy and Hulme in 1954. The A15 type compound superconductors are important materials for practical use (Lee, 2001). The stoichiometry (the relative composition of constituent atoms mandated by the ideal crystal structure) of the material of this class is A_3B, where A is one of the transition metals such as Nb, V, Ta or Zr and the B atom comes from the IIIA or IVA of the periodic table and is a metal or a semiconductor, such as Sn, Al, Ga, Ge, In or Si. The A elements are situated at the corners of a cube and the B elements form three orthogonal chains. The basic superconducting properties of various A15 superconductors are shown intable 2.1(Arbman and Jarlborg, 1978).

Table 2.1 Shows Some A15 superconductors

Compound	$T_c(K)$
V_3Ga	16.5
V_3Si	17.1
V_3Ge	6.0
Nb_3Al	19.1
Nb_3Ga	20.7
Nb_3Si	18.2
Nb_3Ge	32.2
Nb_3Sn	18.0

The A15 is necessarily in the stoichiometric ratio of 3:1. For instance, at low processing temperatures the compositions of Nb_3Ga andof Nb_3Al tend to be richer in Nb than the formula indicates though they have 3:1 compositions at a high processing temperature. The T_c values of more than 50 A15 type superconductors have been confirmed so far. The necessary conditions for higher T_c values are a stoichiometric

composition and a highly regular crystal lattice. The T_c increases when these ideal requirements are approached more and more.

2.1.4. Heavy Fermion superconductors

These are contemporary of organic superconductors and were discovered in 1979 by Steglich et al. (1979). They are characterized by low value of T_c for example: CeCu$_2$Si (0.5K), UBe$_{13}$ (0.85K) and UPt$_3$ (0.5K). Their names reflect their important feature: the effective mass is several hundred times greater than that of the mass of a free electron. The superconducting state displays some anomalous properties. In conventional superconductors, the electronic heat capacity decreases exponentially with temperature, where as in heavy fermions superconductors, a power law decrease is observed.

2.1.5. Nitride and Chevrel Compounds

Nitride compounds NbN, has a T_c value exceeding 17K. Other similar compounds, like, TaN, NbC and MoC have T_c values exceeding 10K. NbN is of particular interest from the point of view of its practical use because of its high T_c. the $N(E_F)$ value is not very high and the strong electron-phonon interaction is thought to be the reason for its high T_c (Ashkin et al, 1984).

The Chevrel compound is represented by chemical formula $M_xMo_6S_8$, in which M can be Pb, Sn, Cu, a rare-earth metal or any other metals (Matthias, 1972). The T_c values are lower than that of A15 type compound. Mo_6S_8 forms one cluster, and eight clusters unite loosely via a Pb atom. The distance of the Mo atoms inside

the cluster(0.26-0.28nm) is shorter than the distance between Mo atoms outside the cluster (0.387nm). Therefore, the conduction electrons are localized within the cluster and have a peculiar electronic structure.

2.1.6 Magnesium Diboride superconductor

The highest T_c of the metallic superconductors represented by the A15 type was not improved for a long time. The situation was changed greatly by the discovery of superconductivity in magnesium diboride (MgB_2) in 2001 with a T_c value of 39K (Nagamatsu, 2001). T_c is determined by three factors, θ_D, $N(E_F)$ and V according to equation 1.2. In the investigation of the isotope effect, a T_c change of 1K is observed by substitution of boron [10]B atoms by [11]B atoms in MgB_2 and the existence of strong electron-phonon interaction with B atom was observed (Bud'ko et al, 2001 and Hinks et al, 2001). The critical temperature T_c of MgB_2 lies on or beyond the estimated upper limit of T_c for phonon-mediated superconductivity in the one-band model (Ginzburg, 2000). From a nuclear magnetic resonance (NMR) study (Kotegawa et al, 2001) the symmetry of the Cooper pairs has been confirmed to be of a spin-singlet type

2.1.7 Organic superconductors

These are an unusual class of superconductors, which are insulators in normal state (with very low conductivity). The first organic superconductor (TMTSF)$_2$X was discovered in 1980 by Jerome et al. (Michael et al, 1987 and Jerome, 1980). Where X is monovalent in organic anion. Typical anions are PF_6^-, AsF_6^- and NbF_6^-. The

transition temperature T_c was only 1K. However, in 1990, an organic superconductor (BEDT-TTF)$_2$X with a T_c value of 12K was synthesized. TMTSF works as a donor which supplies the electrons, and TMTSF molecules are piled up in a pillar shape when combining with the ClO$_4$ acceptors that receive electrons.

2.1.8. C$_{60}$-Based superconductors

The C$_{60}$ molecule, which is called a fullerene and is shaped like a soccer ball consisting of 60 carbon atoms, was discovered in 1985 by Harry Kroto and Richard Smalley and the solid composed of these molecules has been found to show conductivity by carrier doping of C$_{60}$ with patassium atoms (Kroto et al, 1985). The first C$_{60}$ superconductor to be discovered was K$_3$C$_{60}$ with T_c=18K (Hebard et al, 1991). Hebard et al. (1991) obtained superconductivity at 18K in K$_x$C$_{60}$. Rb-doped C$_{60}$ produced superconductor with a T_c~28K and the T_c of Cs$_3$C$_{60}$ was the found to be as high as 38K in 1991 by Kelty however the superconducting phase was less stable in Cs doped C$_{60}$ than in K- and Rb-doped superconductors (Ganin et al, 2008).

2.1.9 High Temperature Superconductors (Copper oxides)

These oxide superconductors are defect perovskite like cuprate materials, which were discovered in 1986 by Bednorz and Muller. (Bednorz et al, 1986). These materials have T_c^s as high as 90-125K. (Prior to this, T_c achieved was below 23.2K, corresponding to that of Nb$_3$Ge). Bednorz and Muller discovered high temperature superconductivity (T_c~35) in defect perovskite like oxide material La$_{2-x}$Ba$_x$CuO$_4$. These materials are layered structures in which sheets of copper and oxygen atoms

alternate with sheets of rare- earth (and oxygen) atoms. Soon after, Chu and co-workers discovered the so called 123 oxides of general formula $LnBa_2Cu_3O_{7\text{-}}\sigma$ (Ln=Y, Nd, Sm, Eu, Gd, Dy, Ho, Er, Tm, or Yb) with T_c values in the 90K region (Chu et al, 1987). The discovery of these materials with superconductivity above liquid nitrogen temperature raised much hope and prompted intensive search for new classes of oxides with still higherT_c^s. Two series of compounds belonging to the Bi-Sr-Ca-Cu-O and Tl-Ba-Ca-Cu-O systems have been found to exhibit superconductivity between 60 and 125K (Maedaet al, 1988 and sheng et al, 1988). Mercury based superconductors (Hg-Ba-Ca-Cu-O) were discovered in 1992 by Putilin and Schilling with a T_c value of 130K (Putilinet al, 1993). The highest temperature superconductor (at ambient pressure) is mercury barium calcium copper oxide ($HgBa_2Ca_2Cu_3O_x$) perovskite material possibly 164K under high pressure. (Chu etal, 1993)

All high temperature cuprates possess "defect perovskite layers"except 123 compounds contain rock salt type oxide layers. In the La-based, Y-based, Bi-based, Tl-based, and Hg-based cuprate families, the carriers of superconducting current are electron vacancies or holes (pairs). By contrast, in the HTSC ($La_{2\text{-}x}Ce_xCuO_{4+y}$) discovered by Tokura et al, in 1989 with aT_c value of 25K, the carriers are electron pairs as verified by Hall-coefficient measurement.

**2.2	High-Temperature superconductivity**

High-temperature superconductors have three common characteristics in the context of superconductivity

i.	Compounds that exhibit superconductivity at temperature above 30K.

ii.	Compounds having a transition temperature that is a larger fraction of the Fermi temperature than for conventional superconductors such as elemental mercury or lead.

iii.	Compounds with transition temperature greater than the boiling point of liquid nitrogen (77K or -196°C). This is significant for technological applications of superconductivity (since liquid nitrogen is easily available and inexpensive)

In 1986 the term high-temperature superconductors was first used to designate the new family of cuprate-perovskite ceramic materials discovered by Johannes Georg Bednorz and Karl Alexander Muller. They discovered LaBaCuO with transition temperature of 35K. (Bednorz et al, 1986)

2.2.1 Crystal Structure of high-temperature ceramic superconductors

It has been shown by several groups of scientists that the new HTSCs are structurally flawed members of crystallographic family known as cuprates (Hazen et al, 1987).

The structure (location of atoms) is prerequisite for understanding the physical properties of cuprates. The crystal structure of copper oxides is highly anisotropic. Such a structure describes most physical properties of cuprates. In conventional

superconductors, there are no important structural effects. Cuprates are basically tetragonal and all of them have CuO_2 planes. Superconductivity occurs in the copper-oxide planes. Copper- oxide planes are always separated by layers of other atoms such as Bi, Y, Ba, La, Hg etc., which provide the charge carriers into the copper-oxide planes. These layers are often called charge reservoirs. Critical temperatures depend on the chemical compositions, cations substitutions and oxygen content.

2.2.2 Perovskite structure

Perovskites are ceramics (solid materials combining metallic elements with non-metals, usually oxygen) that have a particular atomic arrangement. In their ideal form, described by generalized formula ABX_3, they consist of cubes made up of three distinct chemical elements (A, B and X) that are present in the ratio 1:1:3. The A and B atoms are cations (positive) and X atoms are anions (negative). An A atom, the largest of the two kinds of metals, lies at the centre of each cube, B cations occupy all the eight corners and the X anions lie at the midpoints of the cube's twelve edges as shown in figure 2.1.
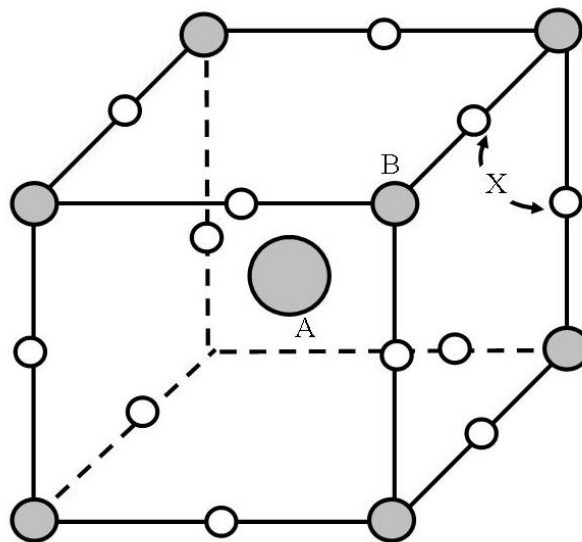
Figure 2.1. The perovskite structure of ABX_3 Kumar (2010)

2.2.3 Early Oxide Superconductors

Many oxide superconductors were investigated before the discovery of high temperature cuprate superconductors. $LiTi_2O_4$ with $T_c \sim 14K$ (Satpathyet al, 1987), $SrTiO_{3-x}$ ($\sim 0.5K$) and $BaPb_{1-x}Bi_xO_3$ ($\sim 13K$) (Koonce et al, 1967 and Sleight et al, 1975). These compounds created acute interest in study of electronphonon-interaction. $BaPb_{1-x}Bi_xO_3$ and $Ba_{1-x}K_xBi_xO_3$, were later discovered, and have the $BaBiO_3$ structure as the host crystal. It is called the perovskite structure and it is represented by the general chemical formula ABO_3, where A and B are metals. Substituting the Bi site of $BaPb_{1-x}Bi_xO_3$ with Pb will give a disorder to the network of conduction. Therefore, the$Ba_{1-x}K_xBi_xO_3$ system in which the Ba^{2+} does not take part directly in the conduction is substituted by K^+ ion. It was investigated and observed that $Ba_{1-x}K_xBi_xO_3$ metalizes when x=0.4 and simultaneously becomes a superconductor with $T_c \approx 30K$ (Cavaet al, 1988).

2.2.4 The structure of $YBa_2Cu_3O_{7-x}$

These compounds are described as distorted, oxygen deficient multi-layered perovskite structure. This compound has $T_c > 90K$ and has orthorhombic structure. The structure has two Cu-O sheets in the ab plane and Cu-O chains along b-axis. B is the metallic cation Cu (small radius), surrounded by six oxygen ions occupying site X. The cation site A is occupied by yttrium (larger radius than B). By eliminating oxygen atoms from the ideal perovskite lattice, $YBa_2Cu_3O_7$ is obtained and its unit cell contains: a layer of Cu-O having copper surrounded by four oxygen ions, a layer of BaO, a layer of Cu-O surrounded by five oxygen ions forming a polyhedron and a

layer of yttrium short of four oxygen. The Cu-O chains are along the b-axis and the oxygen atoms in these chains are responsible for superconductivity. In $YBCO_6$ there are no Cu-O chains, and the compound is an antiferromagnetic insulator. The role of yttrium is very minor, just to hold the two CuO_2 layers apart. In the crystal, Y has a valence of +3. The replacement of Y by many of lanthanide series of rare- earth elements causes no appreciable change in superconducting properties. Outside the layer CuO_2-Y-CuO_2 sandwich are BaO planes and Cu-O chains. Ba has a valence of +2 in the crystal. The Cu-O distance in the chains is ~1.9Å. At an oxygen content of 6.0, the lattice parameters a≠b, and the unit cell is orthorhombic. The increase in oxygen content causes the unit cell to square symmetry, i.e. a=b. The crystal structure becomes tetragonal at low temperatures. At an oxygen content of 6.4, antiferromagnetic long-range order disappears and the superconducting phase starts developing. The T_c remains around 90K from x=0 to x≈0.2. For x=1.0, there are no chain oxygen atoms and T_c is zero. The maximum T_c is achieved at doping level of about 6.95 (the optimal doping). Unfortunately, it is not possible to explore the phase diagram above the oxygen content of 7.0, since the Cu-O chains are completed. $YBCO_7$ is a stoichiometric compound with the highest T_c. Figure 2.2shows the structure of YBCO (Greenwood, 1997).
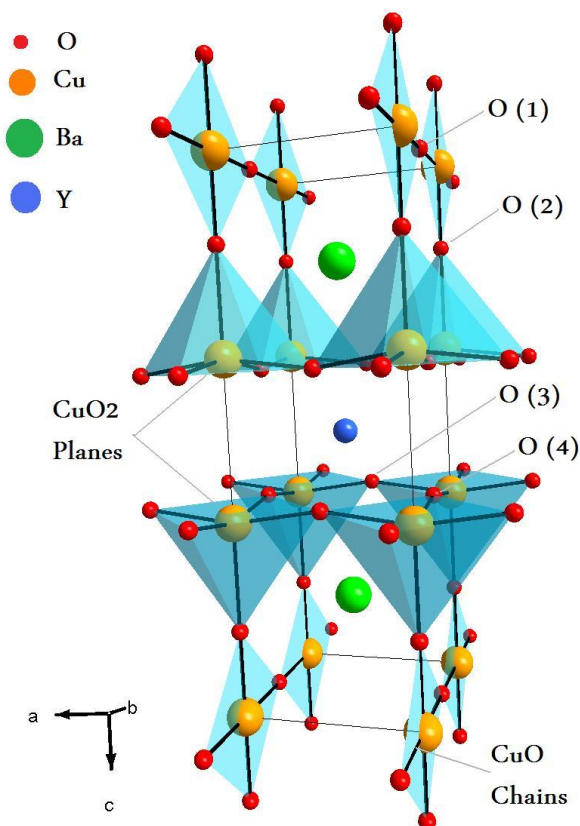
Figure 2.2: Structure of a YBCO system (Greenwood, 1997).

2.2.5 The structure of $La_{2-x}M_xCuO_4$

Unlike YBCO (which have their structure derived from ideal perovskite by ordered removal of oxygen atoms), La-based, Bi-based and Tl-based cuprates have structures derived from ideal perovskite structure through an intergrowth phenomenon. M is the alkaline earth element e.g. Sr or Ba. It is substituted on the lattice. $La_{1.85}Sr_{0.15}CuO_4$ has tetragonal K_2NiF_4 type of layered perovskite structure. The structure can be viewed as a stacking of $-CuO_2$-LaO-LaO-CuO_2-LaO-LaO-CuO_2-. The conducting CuO_2 planes are~6.6Å apart. $La_{2-x}M_xCuO_4$ shows the highest T_c around a critical value of x=0.15 for Sr and x=0.2 for Ba with T_c of 30K and 35K

respectively. $LaCuO_4$ is antiferromagnetic, as the concentration x of Ba^{2+} ions increases the holes that become carriers are implanted into the CuO_2 layers and concurrently increases the value of T_c to a maximum of 38K. However, if the substitution continues the carriers start to overdope and T_c decreases. If Sr^{2+} ions are used instead of Ba^{2+} ions to replace the La^{3+} ions, a high-T_c superconductor is also produced. As for $Nd_{2-x}Ce_xCuO_4$ in which Nd^{3+} ions are substituted by Ce^{4+} ions, the carriers of this material are electrons instead of holes. Superconductivity with T_c=25K is achieved when the concentration of Ce^{4+} ions are x=0.14, and T_c disappears with additional Ce^{4+} ions.

2.2.6 The Structure of Bi-Based Cuprate Superconductors

Bi-based superconductors were discovered by Michel and coworkers in 1987 (Michel et al, 1987) with superconductivity between 7 and 22K in rare-earth-less material Bi-Sr-Cu-O. When Ca was added to Bi-Sr-Cu-O tenary by Maeda et al (1988), the value of T_c rose to 85K in $Bi_4Sr_3Ca_3Cu_4O_{16}$ system (Jarascan et al, 1988 and Sunshine et al, 1988). The value of T_c was further increased to 110K in $Bi_2Sr_2Ca_2Cu_3O_{10}$ (Gao et al, 1994).

The crystal substructure can be viewed as a three dimensional parking of $Bi_2Sr_2Ca_4Cu_2O_8$ slabs along the c-axis, with the main feature being the presence of two Bi-O layers separated by 3.0 Å and shifted, with respect to each other (crystallographic shear) along the diagonal direction of the perovskite sub-cell (Tarascan, 1988). The three phases of Bi-Sr-Ca-Cu-O can be represented by the general formula $Bi_2Sr_2Ca_{n-1}Cu_nO_y$ (n = 1, 2 and 3) and have a pseudo-tetragonal

structure. For $Bi_2Sr_2Ca_4Cu_2O_8$ a stacking sequence is Bi-Sr-Cu-Ca-Cu-Sr-Bi and in $Bi_2Sr_2Ca_2Cu_3O_{10}$ the stacking sequence is Bi-Sr-Cu-Ca-Cu-Ca-Cu-Sr-Bi. The BSCCO system is superior over the YBCO because it is resistant to water or humid atmosphere and has the advantage of oxygen stability. Another advantage of BSCCO materials relates to the fact that Bi-O layers are Vander Waal bonded, these materials can easily be rolled. This property has been utilized successfully for tape-casting and its texturing.

2.2.7   The Structure of Tl-Based Cuprate Superconductors

Tl-based superconductors were discovered by Sheng and Herman in 1988 (Sheng et al, 1988) by substituting non-magnetic trivalent Tl for R in R-123, where R is a rare earth metal. By reducing the reaction time to a few minutes for overcoming the high-volatility problem associated with Tl_2O_3, they dedicated superconductivity above 90K in $TlBa_2Cu_3O_x$ samples. By partially substituting Ca for Ba they discovered a $T_c \sim$ 120K in the multiphase sample of Tl-Ba-Ca-Cu-O. By varying the chemical composition of Sheng and Herman's sample to $TlBa_2CaCu_2O_8$ and $Tl_2Ba_2Ca_2Cu_3O_{10}$ by Hazen et al. (Hazen et al, 1988 and Parkin et al, 1988) it increases the superconducting T_c to 125K. The crystal structure of thallium-based superconductors is given by the general formula $Tl_mBa_2Ca_{n-1}Cu_nO_{2(n+1)+m}$ (m=1,2 and n=1−6).

2.2.8   The Structure of Hg-Based Cuprate Superconductors

Hg-based superconductors were discovered by Putillin and co-workers in 1992 (Putillin et al, 1993) and they found that $HgBa_2CuO_x$ compound with only one CuO_2 layer showed a T_c up to 94K. In 1993 Schilling and co-workers reported superconductivity up to 133K in $HgBa_2Ca_2Cu_3O_x$ after increasing the number of CuO_2 layers (Schilling et al, 1993). The transition temperature of $HgBa_2Ca_2Cu_3O_x$ was further increased to 153K by application of a quasi-hydrostatic pressure of 150K-bar (Chu et al, 1993).

The structural arrangement of $HgBa_2CuO_{4+\delta}$ is similar to that of $TlBa_2CuO_5$, except for oxygen stoichiometry of the HgO_δ and $TlO_{1-\delta}$ layers respectively. For the former, δ is very small and for the latter, $TlO_{1-\delta}$ layer is only slightly oxygen depleted. These different requirements for attaining the optimal concentration of holes (carriers) are due to different preferred coordination geometries of the Tl^{3+} and Hg^{2+} cations. The rare-earth based Hg: 1212 compounds were not found to be superconducting because the hole concentration in these phases was not high enough to induce superconductivity. When trivalent rare-earth cations are replaced by divalent Ca^{2+} the transition temperature was above 120K in $HgBa_2CaCu_2O_{6+\delta}$ (Putillin et al, 1993).

Table 2.2 shows the Number of Cu-O planes for some oxides (Chu C.W. et al, 2007)

Formula	Notation	Tc (K)	Number of Cu-O/unit cell	Crystal structure
$YBa_2Cu_3O_7$	123	92	2	Orthorhombic
$Bi_2Sr_2CuO_6$	Bi-2201	20	1	Tetragonal
$Bi_2Sr_2CaCu_2O_8$	Bi-2212	85	2	Tetragonal
$Bi_2Sr_2Ca_2Cu_3O_6$	Bi-2223	110	3	Tetragonal
Tl_2Ba_2CuO6	Bi-2201	80	1	Tetragonal
$Tl_2Ba_2CaCu_2O_8$	Tl-2212	108	2	Tetragonal
$Tl_2Ba_2Ca_2Cu_3O_{10}$	Tl-2223	125	3	Tetragonal
$Tl_2Ba_2Ca_3Cu_4O_{11}$	Tl-2234	122	4	Tetragonal
$HgBa_2CuO_4$	Hg-1201	94	1	Tetragonal
$HgBa_2CaCu_2O_6$	Hg-1212	128	2	Tetragonal
$HgBa_2Ca_2Cu_3O_8$	Hg-1223	134	3	Tetragonal

2.2.9 Characteristics of High Temperature Superconductors

Some of the common characteristics of oxide high temperature superconductors are as follows:

1) They have their structure derived from perovskite structure (therefore termed as defect perovskite structure), either through an intergrowth phenomenon or by an ordered removal of oxygen atoms.

2) They have layered crystal structure consisting of one or more CuO_2 layers. Each copper atom in a $Cu-O_2$ plane is strongly covalently bonded, in a nearly square-planar arrangement, with four numerical atoms at a distance of 1.9 Å.

3) Copper is present in mixed valence state involving a partial oxidation of Cu^{2+} to Cu^{3+}.

4) There is a charge transfer, to and from the CuO_2 layers, which is induced by doping near the metal-insulator phase boundary (in the phase-diagram) existing in all oxide high T_c superconductors.

5) The sign of Hall coefficient is positive, indicating that the charge carriers are holes in all oxide HTSCs, except $Nd_2{-}xCe_xCuO_4$, which is an electron superconductor. Hall coefficient for magnetic field H parallel to ab plane is much smaller than H parallel to the c-axis.

6) When rare-earth (RE) ions replace Y in $YBa_2Cu_3O_7$, T_c remains unchanged and most of the transport properties are unaffected. However, the specific heat data of (RE) $Ba_2Cu_3O_7$ compounds, which are within 2% of the $YBa_2Cu_3O_7$ for T $>T_c$ show drastic differences at low temperatures. This arises due to the magnetic interactions between the paramagnetic ions as well as between these ions and the crystal field. This establishes that superconductivity and magnetism can co-exist in the RE compounds and RE ions do not participate in superconductivity.

7) The normal state transport properties are highly anisotropic. In YBCO, there is a linear dependence of the ab plane resistivity (ρ_{ab}). But the c-axis resistivity (ρ_c) shows a semi-conducting dependence ($\propto 1/T$) for less oxygenated samples and ($\propto T$) for well oxygenated samples. $\rho_c/\rho_{ab} \sim 30$ at room temperature. Similar anisotropic behaviour is observed in other HTSCs.

8) All of them are type II superconductors with two critical magnetic fields. The lower critical field H_{c1} and upper critical field H_{c2} which are highly anisotropic.

9) The two fundamental superconductivity parameters viz. the coherence length ξ and penetration depth λ are also highly anisotropic. Further, the magnitude of coherence length is quite small as compared to that of conventional superconductors.

10) The value of $2\Delta(0)/k_B T_c$ is smaller for tunneling of pairs perpendicular to ab plane (i.e. its range is 3.8–4.0) compared to tunneling of pairs parallel to ab plane (i.e. its range is 5.8–6.0).

11) The low temperature specific heat, C, of HTSCs in the superconducting phase is due to three contributions: $C = \alpha T^{-2} + \gamma T + \beta T^3$. The first term gives the Schottky-like anomaly and arises from magnetic impurities. The second is a linear contribution similar to that for free electrons in a metal. The third is Debye contribution from the lattice. The absence of the exponential dependence of the electronic specific heat (expected on the basis of the BCS theory) is a major departure from the properties of the conventional superconductors.

12) The phononic mechanism of superconductivity (BCS theory) has certain limitations in theoretically explaining the mechanism of superconductivity in the cuprate high temperature superconductors. Various other mechanisms have been proposed (e.g. Anderson's RVB Model, Schrieffer's spin-bag model, Bipolaron model, etc.). But still no suitable mechanism is able to

explain satisfactorily various normal-state and superconducting properties of these materials.

2.2.10 Resemblance Between HTSC and Conventional Superconductors

1) Superconducting state is made up of paired carriers.

2) Presence of a true gap ($\Delta(\kappa) \neq 0$ for all values of κ) where κ is the Ginzburg-Landau parameter.

3) Jump in specific at $T = T_c$

4) The pair wave function has s-wave symmetry.

5) Presence of a Fermi-surface.

2.2.11 Unusual Properties of HTSCs

1) Small coherence length ξ (This reduces the pinning energy implying weak pinning)

2) Large penetration depth λ (This softens the flux line lattice (FLL))

3) Large energy gap (Δ)

4) Large anisotropy $(cf. \xi_{ab} > \xi_c)$ (This is due to layered structure).

5) Small Fermi energy (E_F).

6) High $T_c (\sim 90 \ to \ 130K)$

7) Smaller carrier concentration. There are only ≤ 5 pairs per coherence volume as compared to 10^4 pairs per coherence volume for BCS conductor)

8) High $H_{c2}(= \Phi_0/2\pi\xi^2)$ which is anisotropic and much larger when applied parallel to the planes than when applied perpendicular to the planes ~ 1 M Gauss (for YBCO), which is $3 - 5$ times the fields available presently.

9) Heat transport dominated by lattice $(k_{el} << k_{lat})$.

10) The jump in heat capacity is not sharp.

11) a)   Sound velocity (elastic constants) is dramatically affected at T_c (unaffected for conventional superconductors).

b) Presence of low-lying optical phonon modes.

2.3 Theories of Superconductivity

The discovery of superconductivity aroused an enormous interest. Many physicists tried their hands at explaining the disappearance of electrical resistance and other features of the superconducting state. A number of important phenomenological theories were proposed which allowed the phenomena and its various properties to be explained.

2.4 Theories of Conventional Superconductors

Several theories have been put forward by scientists to try and explain the mystery of superconductivity and some of them are presented in the subsections below.

2.4.1 Two-Fluid Model

In 1934, Gorter and Casimir proposed the "two-fluid" model. This model assumes that the electron liquid in a superconductor can be imagined as a combination of two liquids: "normal" and "superconducting." The properties of the "normal" component are identical to those of the electron system in a normal metal, and the "superconducting" component is responsible for the anomalous properties. With decreasing temperature, the "superconducting" fraction grows while the density of the "normal" component decreases and finally vanishes at zero temperature. The superconducting component is responsible for the persistent currents, whereas the electronic heat capacity and thermal conductivity are governed by the "normal' fraction. The two-fluid model proved to be a useful concept only for analyzing the thermal properties of superconductors. (Gorter and Casimir, 1935).

Vortices were discovered by Shubnikov and coworkers in 1937 (Shubnikov et al, 1937). They found an unusual behaviour for some superconductors in external magnetic fields. They discovered the existence of two critical magnetic fields for type-II superconductors and the new state of superconductors is known as mixed state or Shubnikov's phase.

The isotope effect was found in 1950. A study of different superconducting isotopes of mercury established a relationship between the critical temperature T_c and the isotope mass M as given in equation 2.3(Reynolds et al, 1950 and Maxwell, 1950).

$$T_c M^{1/2} = \text{constant} \qquad\qquad (2.3)$$

2.4.2 Ginzburg-Landau Theory

In 1950, Ginzburg and Landau proposed the Ginzburg-Landau theory based upon the Landau theory of second-order phase transitions, the theory played an important role in understanding the physics of superconducting state.

The Ginzburg-Landau theory made it possible to study the behavior of superconductors in strong magnetic fields. At first, it may seem that superconducting current is ideally suited for the production of strong magnetic fields. Indeed, when a normal conductor is used, a large part of the power goes into thermal losses. In order to obtain very strong fields, very high currents are required, but I^2Rt heating can lead to melting of the material. There is no such danger in superconductors due to the absence of electrical resistance. It would seem, therefore, that we should be able to obtain magnetic fields of any desired magnitude by simply turning up the superconducting current. Unfortunately, as soon as the field becomes equal to H_c, superconductivity is destroyed. Nevertheless, a class of substances has been found that remain superconducting in strong magnetic fields and at intense currents. (Ginzburg and Landau, 1950).

By using Ginzburg-Landau theory Abrikosov theoretically found vortices and thus explained Shubnikov's experiments, suggesting that Shubnikov's phase is a state with vortices that actually forms a periodic lattice (Abrikosov, 1957).

2.4.3 Einstein's Theory

Einstein pointed out an analogy between superconductivity and ferromagnetism. In ferromagnetics, the collective interaction between electrons leads

to spontaneous magnetization which is stable with respect to thermal motion. He attempted to construct a theory in which the collective interaction similarly leads to a formation of certain entities (Einstein called them "clouds") moving without friction. Also in 1947, Heisenberg attempted to explain superconductivity by analyzing the Coulomb interaction in a many electron system such as a metal. He considered a free-electron gas. (Eliashberg,1961).

2.4.4 Microscopic Theory (BCS Theory)

A systematic theory of superconductivity, which explained the nature of this phenomenon, was formulated in 1957 by Bardeen, Cooper, and Schrieffer (and this theory is referred to as BCS Theory). The mystery of superconductivity was solved, and the formulation of the theory brought further progress in the field. In the explanation of the phenomenon of superconductivity, the interaction between electrons and the crystal lattice was taken into account. It turned out that this interaction leads to attraction between the electrons in a superconductor. At first glance, this seems strange, since we are used to seeing electrons, having the same charge, repel each other. In fact, there is no contradiction with the laws of physics here. Of course, two electrons in a vacuum will repel each other. We are not considering, however, the problem of two isolated electrons. The electrons are located in a medium, that is, inside a crystal, and the presence of a medium can change the sign of the interaction. It turns out that the interaction between the electrons and the lattice leads to a certain effective interaction between the electrons. The nature of this interaction is as follows. An electron moving in a metal deforms, or polarizes, the

crystal lattice by means of electric forces. The displacement of the ions in the lattice caused in this way affects the state of the other electron, since the latter now finds itself in the field of the polarized lattice with a somewhat altered structure. This results in an effective attraction between the electrons.

The appearance of the attractive force can be visualized as follows. As a result of the deformation of the lattice, an electron is surrounded by a "cloud" of positive charge which is attracted to the electron. The magnitude of this positive charge can exceed the electron charge. Then this electron, together with the surrounding "cloud," represents a positively charged system, which will be attracted to another electron.

At high temperatures, sufficiently intense thermal motion pushes particles apart from each other and washes away the ion "coat," which effectively reduces the attractive forces. At low temperatures, however, these forces play a very important role.

The crystal lattice is thus the medium which makes the dielectric permit-tivity in a superconductor negative.

The appearance of the additional interelectron attraction can be described in quantum terms as well. Let us consider a metal at T=0K. Its crystal lattice is not at absolute rest, but executes so-called "zero-point" vibrations, which exist due to the quantum-mechanical uncertainty principle and correspond to the ground state of a harmonic oscillator. An electron moving in the crystal disrupts the state of these zero point vibrations and excites the lattice. When the lattice returns into its ground state, it radiates energy that is absorbed by another electron. The excited state of the crystal lattice is described in terms of sound quanta-phonons. Therefore, the process

described above can be visualized as the emission of a phonon by another electron. This exchange of phonons is what leads, in the quantum picture, to the additional attraction between electrons.

At low temperatures, this attraction in a number of materials (these are superconductors) prevails over the Coulomb electron repulsion. Here the electron system turns into a bound unit, and finite energy must be expended in order to excite it. The energy spectrum of the electron system (we stress that we are referring not to the energy of individual electrons, but to the energy of the entire system of bound electrons, treated as a single unit) in this case will not be continuous. The excited state of the electron system is separated from the ground state by an energy interval.(Berdeen et al, 1957).

2.4.5 Other Theories From 1957 to 1986

Quantum-mechanical barrier of Cooper pairs through a thin insulating barrier (on the order of a few nanometers thick) between two superconductors was theoretically predicted by Josephson (1962). The Josephson's predictions were confirmed within a year and the effects are now known as Josephson's effects. They play a special role in superconducting applications. For example it led to development of very sensitive detectors and of compact, fast and efficient memory units for computers e.g. SQUIDS (superconducting quantum interference devices).

In 1984 the soliton (or bisoliton) model of superconductivity was used by Brizhik and Davydov in order to explain superconductivity in organic quasi-one-dimensional conductors (Brizhik et al, 1984).Schmitt-Rink and Varma in 1986

considered the mechanism of superconductivity in heavy fermions based on the exchange of antiferromagnetic spin fluctuations (Miyakeet al, 1986). The calculations showed that the anisotropic even-parity pairings are assisted and the odd-parity as well as the isotropic even-parity are impeded by antiferromagnetic spin fluctuations.

2.5   Theories of High Temperature Superconductors

After the discovery of high temperatures superconductors in 1986 there is a lot of experimental data that cannot be explained by the BCS theory. A number of theories have been proposed as possible explanation of HTSC. Most of these theories require that there should be an attractive interaction between the charge carries resulting in the formation of pairs which act as bosons, and can undergo Bose-Einstein condensation. The proposed theories fall into the following three main categories:

(i)   Interaction through phonons (Lattice vibrations)

(ii)   Interaction through charges (Charge fluctuations)

(iii)   Interaction through unpaired spins (Spin fluctuations)

2.5.1 The Bipolaron Theory

In the Bipolaron theory, a Polaron is defined as a self-trapped electron, andBipolaron is a bound pair of electrons with a cloud of phonons. The assembly of these bound pairs can undergo superconducting transition at temperatures belowthe Bose-Einstein condensation temperature $T_c$given by,

$$k_B T_c = 3.3 \hbar n^{2/3}/m \qquad\qquad (2.4)$$

where n is the number of density of pairs, and m is the effective mass of each pair.

2.5.2 The Exciton Theory

In the Exciton theory, Excitons are bound states of electron-hole pair created by electrostatic interaction between an electron in the excited state and a hole in the ground state. Oxides superconductors have a layered structure and thus a multiband nature of electron spectrum. It is therefore highly probable to have excitons. Since, here the energy responsible for coupling is of the order of electron energies, much higher T_c can be obtained. Some of the excitons models are:

i. Plasma excitations which have a quasi-two-dimensional electronic spectrum which give rise to the appearance of weakly damped acoustic plasmons.

ii. Collective electron excitation connected to copper-oxygen charge transfer.

2.5.3 The Spin-Bag Theory

Schrieffer in the spin-bag theory, proposed a model in which boson excitations are responsible for superconducting pairing in copper oxide high $- T_c$ compounds. When a mobile hole passes through the CuO_2 lattice, it creates a region of local depression in which copper spins are aligned anti-ferromagnetically. When another hole passes through this region, it gets attracted to this region of lower potential energy resulting in the appearance of a magnetic Polaron that moves with a deformed cloud. High- Tc and wave pairing are conditioned by a strongly anisotropic region due to anti-ferromagnetic spin fluctuations.

2.5.4 Van-hove Theory

Friedel in the theory of van-hove anomaly, proposed that superconductivity is due to electron-phonon coupling of delocalized carriers. Since the carriers are confined to the CuO_2 planes, high $- T_c$ super-conductors exhibit quasi two dimensional Fermi surface. The band structure for holes leads to electronic density of states at or very near the Fermi surface which has van Hove singularity. This logarithmic density of states is defined as,

$$D (E) = D (E_F) \log|\omega/E| \tag{2.5}$$

where the width ω is the characteristic energy for two dimensional band. According to Newns et. al., (Newns, 1992) the critical temperature T_c is given by,

$$k_B T_c = 1.36\omega exp \left[-\sqrt{(2/\lambda)}\right] \tag{2.6}$$

where: $\lambda = VD (E_F)$. Thus the temperature T_c increases because the width ω is of electronic nature which is greater than the phonon energy. The van Hove anomaly in electronic spectrum leads to anomalous isotope effect.

2.5.5 The Resonating Valence Bond (RVB) Theory

In the resonating valence bond (RVB) theory, a Quantum spin liquid or singlet liquid state is called a Resonating Valence Bond State. Anderson found that the whole wealth experimental results on the so-called high – Tc superconducting compounds could not fit in honest way to conventional BCS theory. The departures were in two fronts. The first one is that high- T_c superconductivity is not due to phonon-induced pairing of electrons. The second and perhaps the most important one is that in these superconductors, superconductivity arises not from Cooper pair condensation but of

condensation of new quasi-particles of +ve charge which are now called holons (Kotliar, 1988).

Anderson refers to ceramic superconductors as, strange insulators, strange metal and strange superconductors. Superconducting transition temperature T_c is generally large, of the order of 92K and above. There are indications of unstable superconductivity even at room temperatures. The superconductor-normal metal tunneling is anomalous. There is a strong ultrasonic attenuation and velocity of sound anomaly. The infrared absorption is very different from the BCS compounds. Wide discrepancies are there in the gap measurements obtained from different experiments such as tunneling infrared absorption.

The remarkable fact is the vicinity of the insulating phase to the superconducting phase. At very low temperatures the system directly goes from an insulator to a superconductor.

It was the inelastic neutron scattering in La_2CuO_{u-y} that had shown a clear indication for the presence of a quantum spin (called a RVB state liquid). Anderson generalized Pauling's theory of resonant valence bond to make it relevant to high-T_c oxide compounds. In this model, valence electrons are bounded singlet anti-ferromagnetic pairs (Magnetic singlet pairs) which become mobile as in a liquid in the presence of mobile holes. RVB is characterized by a system of singlet states for pairs of electrons on the lattice sites i and j; described by the order parameter for holons.$B_{ij}=\langle b_i^\dagger b_j \rangle$. The order parameter for spinons is,$\Delta_{ij}=\langle c_{i\alpha}^\dagger c_{j-\alpha}^\dagger - c_{i-\alpha} c_{j\alpha} \rangle$. Where α and $-\alpha$ are the spin indices, $c_{i\alpha}^\dagger$ and $c_{i\alpha}$ are the fermion creation and annihilation operators:Δ_{ij} is the spinon pairing amplitude, while $b_i^\dagger$ and b_i are the

creation and annihilation operators for the bosons which are charged quasi-particles without spin and are called holons.Superconductivity is assumed to be due to:

i.   Condensation of the holons with $\langle b_i^\dagger b_j \rangle \neq 0$. Pairing is by interlayer tunneling of holons.

ii. Tunneling of pairs of electrons between the layers under the condensation of spinon pairing amplitude $\Delta_{ij} \neq 0$.

2.5.6   Other Theories on High Temperature Superconductors

By analyzing the layered structure of cuprates, (Kresin and Wolf, 1987)proposed a model of high temperature superconductivity based on the existence of two gaps: superconducting and induced. Different experiments performed thereafter have indeed demonstrated the existence of two gaps, although they both have the superconducting origin.Gor'kov and Sokol proposed the presence of two components of two itinerant and more localized features in cuprates in 1987 (Gor'kov et al, 1987). This kind of microscopic and dynamical phase separation was later rediscovered in other theoretical models.

Also in 1987, Anderson proposed a model of superconductivity in cuprates, in which pairing mechanism and the mechanism for the establishment of phase coherence are different (Anderson, 1987). Later in early 1990s, proceeding from Anderson's suggestion that in cuprates the pairing mechanism and the mechanism for the establishment of phase coherence are different, a few theorists autonomously proposed that, independently of the origin of pairing mechanism, spin fluctuations mediate the long-range phase coherence in cuprates. It turned out that this suggestion

was correct.Davydov in 1988, suggested that high-T_c superconductivity occurs due to the formation of bisolitons as it does in organic superconductors (Davydov, 1988)

The pseudogap above T_c (Phillips, 1989) was observed in 1989 in nuclear magnetic resonance (NMR) measurements. The pseudogap is a partial energy gap, a depletion of the density of states above the critical temperature (Warrenet al, 1989). In 1990, Davydov presented a theory of high-T_c superconductivity, based on the concept of moderately strong electron-phonon coupling which results into perturbation theory being invalid (Davydov, 1990 and1991). The theory utilizes the concept of bisolitons, or an electron (or hole) pairs coupled in a singlet state due to local deformation of the –O-Cu-O-Cu- chain in CuO_2 planes. Alexandrov and Mott in 1994,pointed out that, in cuprates, it is necessary to distinguish the "internal" wave function of Cooper pairs and the order parameter of the Bose-Einstein condensate, which may have different symmetries (Alexandrov et al, 1994).

In 1995, Emery and Kivelson emphasized that superconductivity requires pairing and long- range phase coherence (Emery et al, 1995). They demonstrated that, in cuprates, the pairing may occur above T_c without the phase coherence. In the same year 1995, Tranquada and coworkers found the presence of coupled, dynamical modulations of charges (holes) and spins in Nd-doped $La_{2-x}Sr_xCuO_4$ (LSCO), from neutron diffraction (Tranquada et al, 1995). In LSCO, antiferromagnetic stripes of copper spins are separated by periodically spaced quasi-one-dimensional domain walls to which the holes segregate. The spin direction in antiferromagnetic domains rotate by 180^0 on crossing a domain wall.

In 1997, Emery, Zachar and Kivelson presented a theoretical model of high-T_c superconductivity (Emery et al, 1997). It turned out that the model is incorrect (there is no charge-spin separation in cuprates); however, it is the first model of high-T_c superconductivity based on presence of charge stripes in CuO_2 planes.

Chakraverty et al, (1998) attempted to prove that the theory of bi-polaron superconductivity of HTSC contradicted with experiments and was theoretically discrepant (Chakraverty et al, 1998). In answer, Alexandrov (Alexandrov, 1999) also stated contrary opinion, namely: the negation of the bi-polaron superconductivity of HTSC is the result of erroneous approximation for energetic spectrum of bi-polaron and erroneous application of the bi-polaron theory carried out by Chakraverty et al.Based on two-zone model, he obtained a formula for T_c, which was free from adjusted parameters and included besides basic constants the concentration of carriers,$n,$ and penetration depths of magnetic flux λ_{ab} and λ_c along two mutually perpendicular crystallographic directions. The substitution of test values of n, λ_{ab} and λ_c (for Y-123) estimated $T_c \sim$ 100K. It proves self-consistency of the bi-polaron approach and testifies HTSC to be in the regime of Bose-Einstein condensation.

Analysis of tunneling and neutron scattering measurements in 1999, showed that, in $Bi_2Sr_2CaCu_2O_{8+x}$ (Bi2212) and $YBa_2Cu_3O_{6+x}$(YBCO), the phase coherence is established due to spin excitations (Mourachkine, 1999 and2001) which cause the appearance of the so called magnetic resonance peak in inelastic neutron scattering spectra (Rossat-Mignod et al, 1991).Tunneling measurements in 2001 provided evidence that, quasi-particle peaks in tunneling spectra obtained in Bi2212 are caused

by condensed like soliton excitations which form the Cooper pairs (Mourachkine, 2001).

In 1999, Cronstrom and Noga determined a new solution of BCS equations in approximation of mean field, which pointed to the existence in thin superconducting films (or superconducting bulks with layered structure) of type-III phase transitions (Cronstrom and Noga, 2001). The critical temperature of this transition increases at decreasing of the layer thickness and is independent of isotope mass. The electronic heat capacity is a continuous function of temperature, but has discontinuity of derivative.

In 1999, Leggett defined a very simple dependence, $T_c(n)$ for "calcium" HTSC (where n is the number of CuO_2 layers per elementary cell): $T_c(n) = T_c(1) + T_0(1 - 1/n)$, where T_0 is the known constant for each Bi, Hg and Tl family, in which the CuO_2 layers are separated by calcium layers(Legget, 1999). In particular, it is followed from this formula that $[T_c(3) - T_c(2)]/[T_c(2) - T_c(1)] = 1/3$, which agrees with test data$0.25 - 0.28$ and$0.25 - 0.34$ for HTSC on the basis of Hg and Tl, respectively.

In 2000, Tang measured the critical temperature, T_c, of ultra-thin HTSC films $YBa_2Cu_3O_7$ depending on their thickness d. It has been observed approximately linearly on d a diminishing of T_c with decreasing of the film thickness at $d<10$nm (Tang, 2000). The dependence $T_c(d)$ is well described by the empirical formula:$T_c = T_{c0} (1 - d_m/d)$,where$T_{c0} = 90$K and$d_m = 1.56$nm. The critical thickness, d_m, is near to the thickness of one elementary cell along c-axis that supports quasi-2D nature of HTSC superconductivity.

In 2001, Kivelson proposed the following way for increasing of T_c: it is necessary to create multi-layer systems with different concentrations of carriers in various layers, so the layers with low concentration of carriers provide their coupling, but the layers with high concentration of carriers guarantee phase rigidity (Kivelson, 2002). Maximal critical temperature of HTSC is found by competition of two effects: (i) the coupling interaction weakens at increasing of the charge carrier concentration, x, that is connected with properties of doped Mott's dielectric, but (ii) the density of super-fluid component, which controls the system rigidity in relation to phase fluctuations, increases with growth of x. Thus, optimal T_c is reached at the boundary of the region with prevalence of the phase alignment and region with prevalence of the coupling interaction.

In the same year 2001, based on tunneling measurements, Mourachkine provided evidence that the quasi particle peaks in tunneling spectra of Bi-2212 crystals are caused by condensed soliton-like excitations, which form the Cooper pairs (Mourachkine, 2001).

In 2002, Cui proposed a possible a responsibility for superconductivity of relativistic attraction of electrons. At least, there are two types of collective movement in superconductors, which can suppress usual Coulomb repulsion of electrons as the attraction component becomes predominant. This movement is caused by combination of electron gas and phonons in conventional superconductors and by itself electron gas (or electron liquid) – in HTSC. The repulsion and attraction between electrons balance approximately each other in majority of matters; therefore, the theory of electron gas (i.e., non-interacting particles) works well. However, the

repulsion predominates over attraction in some materials, and then electron sub-system demonstrates properties directly contrary to superconductivity (Cui, 2002).

In the year 2002, Laughlin showed that cuprate HTSC in undoped state should be considered as no dielectrics, but superconductors with very great gap and extremely small super-fluid density (Laughlin, 2002).Laughlin named these superconductors "gossamer superconductors". In practice, a brittleness of coupled state of this superconductor creates obstacles for stating superconductivity in all volumes. However, he assumed that the wave function of this coupled state can serve as a good starting point for understanding of correlations between Mott's dielectrics and HTSC.

In the year 2002, Khanna and Kirui put forward a theory that explains a mechanism of pairing known as electron-pairing in exotic superconductors. The electronic pairing in exotic superconductors is such that three electrons take part in the superconducting current and that they interact with each other through harmonic forces (Khanna and Kirui, 2002).Two of these electrons form a bound pair while the third one is a polarization electron which hops from one lattice site to another lattice site of similar symmetry. Studies that have been done in photo-induced Raman scattering (Mihailovic et al, 1990) have confirmed that there exists strong anharmonic nature of apical oxygen vibrations. When the spectral function of electron-phonon interactions compared with the phonon spectrum in bismuth compounds it noted that, both low frequency vibrations (buckling mode) and high frequency vibrations (breathing mode) contribute to the electron-phonon coupling (Shimadaet al, 1998).

It is therefore assumed that the polarization electron causes perturbation with respect to the apical oxygen vibrations leading to the contraction of $Cu_p - O_3$ bond. This perturbation is assumed to be of the form $H' = \beta x^3 + \gamma x^4$ where β and γ may or may not depend on temperature. Using anharmonic perturbation, and the non-degenerate many-body perturbation theory, the critical transition temperature for both the buckling and breathing modes were found to be $9.1K$ and $35.5K$ respectively for $La_{2-x}Sr_xCuO_4$ system.

In 2003, Hussey et al. proved an existence of 3D Fermi surface, based on investigations of angle oscillations of magnetic resistance in HTSC $Tl_2Ba_2CuO_{6+\delta}$ (Hussey et al, 2003). Thus, almost a 20-year-old argument about coherency or incoherency of electronic states along the c-axis was solved in favour of coherency. In 2004, Homes et al. obtained the next universal scaling relationship between physical values, characterizing normal and superconducting states of HTSC (Homes et al, 2004): $\rho_s = As_{dc}T_c$ (where ρ_s is the density of super-fluid component, s_{dc} is the static specific conductivity and T_c is the critical temperature), which should be carried out for *all* HTSC, without dependence on the value of T_c, type of carriers (holes or electrons), doping level, crystalline structure and current direction (parallel or perpendicular to CuO_2 planes). In this case, the proportionality factor $A = 120 \pm 25$, if ρ_s is measured in s^{-2}, s_{dc} in $(\Omega\,cm)^{-1}$ and T_c in K. The straight dependence, $\rho_s(s_{dc}T_c)$, includes even the points for low-temperature superconductors Pb and Nb. It covers diapason above of five degree of magnitude on each of the coordinate axes. This empirical dependence is surprising, if taking into account the principally

different character of current transfer in various crystallographic directions (i.e., coherent in *ab*-plane and incoherent along *c*-axis).

In the year 2004, Alexandrov again explained HTSC physics on the basis of bi-polarons mechanism. HTSC properties weakly differ from usual metals, namely: there is standard BCS phenomenon, only Bogolyubov's quasi-particles (Cooper's pairs with *d*-symmetry) transfer current. The magnetic mechanism of superconductivity exists, but as subsequent of electron-phonon coupling. Because constants of electron-phonon are greater than 1, polarons and super-light bi-polarons must arise. In this case, the critical temperature is found as (Alexandrov, 2004)

$$T_c = 1.64[eR_H/(\lambda_{ab})^4(\lambda_c)^2]^{1/3} \qquad (2.7)$$

whereeis electron charge, R_H is Hall constant, λ_{ab} and λ_c are the penetration depth of magnetic field in *ab*-plane and along *c*-axis, respectively.

In 2006, Honma and Hor proposed to distinguish 2D and 3D hole concentration (Honma and Hor, 2006). It is well known that the critical temperature of HTSC is a universal function of this parameter (the hole concentration is usually found by the number of holes per Cu atom in CuO_2 layer). Their analysis shows that T_c is defined by 3D *concentration,* n_h, and universal bell-like dependence takes place just for $T_c(n_h)$.

In this year, Terashima et al. demonstrated experimentally in HTSC a change of the character of the anomaly for the law of electron dispersion (so called "kink") in the vicinity of Fermi level at partial substitution of Cu atoms by Zn and Ni atoms, not much differing in mass, but in other spin states (that may be considered as "magnetic isotope-effect") (Terashimaet al, 2006).

Obviously, the above list of mechanisms and superconductivity theories is not complete. Finally note that beginning from 1987, theorists proposed more than 100 models of high temperature superconductivity, in particular, based on the representations about polarons, plasmons, excitons, solitons, super-exchange and direct interaction between electrons. Today, the intensive discussion of HTSC mechanisms and high critical temperatures, T_c, to being proper for these materials is continued.

Although much progress has been made in understanding the mechanisms that may ultimately lead to the development of a comprehensive theory for the high $-T_c$ superconductivity, the nature of the pairing mechanism that may finally describe the properties of such systems is still unknown and this is still a puzzle to be solved by scientists.

CHAPTER THREE

METHODOLOGY

3.1 Introduction

This chapter presents a detailed description of the techniques used in the formulation

of the theories. It also presents methods of data generation and data analysis.

3.2 The effect of electric and magnetic fields on the HTSC systems.

This section was divided into three parts.

3.2.1 Effect of electric field (*E*).

Superconducting charge carriers flow along CuO_2 planes and Cooper pairs interact

with each other as they flow. The interaction of Cooper pairs and positive ions leads

creation of an electric field that in turn acts on the Cooper pairs. The interaction leads

to perturbation of the system. The Hamiltonian of the system has three parts; the

kinetic energy, potential energy and the perturbation. The Hamiltonian was then

converted into creation and annihilation operators for bosons. On solving the

Hamiltonian using second quantization formalism a final result for the energy gap of

the system was obtained and its effect on the transition temperature of a YBCO

system investigated.

3.2.2 Effect of magnetic field (*H*).

Under this section, a two-dimensional square lattice was considered. When external

magnetic field (*H*) was applied on the lattice cell an electron on a lattice site

underwent two periodic motions under influence of the magnetic field. The ratio of the periodic motions (α) was given by the ratio of the flux through the lattice cell to one flux quantum. Quantum mechanics was used by using the Heinsberg uncertainty principle to determine the value of transition temperature at which Cooper pairs break up and vice versa under influence of an applied magnetic field.

3.2. 3Effect of magnetic flux (Φ).

Under this section, Harper's equation was subjected to second quantization formalism, solved and an expression relating transition temperature (T_c) and magnetic flux (Φ)obtained. The expression was used in calculating the values of magnetic flux for some HTSC systems.

3.3 Research Variables.

The following research variables were considered:

a) Energy gap(Δ).

b) Transition temperature(T_c).

c) Magnetic flux(Φ).

d) Ratio of magnetic flux through a lattice cell to one flux quantum(α).

3.4 Generation of data.

The data tables were obtained when the values of the constants were substituted into equations derived. Using math CAD application software, the resulting expressions were simplified and tables of values generated.

3.5 Data Presentation.

Data generated was presented in tabular form. Graphs were drawn using math CAD application software and conclusions drawn from the graphs.

CHAPTER FOUR

THEORETICAL DERIVATIONS AND CALCULATIONS

4.1 Introduction

The transport properties of cuprates change drastically by the introduction of charge carriers (electrons or holes by doping) to the Cu-O planes. This is done by chemical doping that varies for each family of cuprates. For instance, in the case of LBCO, the chemical doping is done by the substitution of some of the La^{+3} atom by Ba^{+2} which introduces holes to the Cu-O plane. As a rule, each Cu site presents one free electron. But the conduction is suppressed because the strong Coulomb on-site repulsion prohibits two electrons to occupy the same site, leading to the so-called Mott insulator state. In this state, each electron is frozen in a lattice site because it cannot overcome the high energetic double occupancy price. The cuprates also present anti-ferromagnetic state when un-doped (Vaknin, 1987). The second order process of virtual hopping between neighbour sites back and forth leads to an overall reduction of the total energy of the state. This process is only possible if neighbouring electrons have opposite spins, leading the material into an anti-ferromagnetic order. The superconductivity property will arise once we remove some of the electrons, allowing the electrons to hop and therefore destroy the anti-ferromagnetic insulator (AFI) state.

A common feature of all superconductors, both the low and the high temperature superconductors is that the electrons somehow form Cooper pairs. Evidence for Cooper pairing can be obtained from the observation of the magnetic flux quantization (the flux quantization being $h/2e$) (Gough, 1987). The flux

quantization being $h/2e$ and not h/e since Cooper pair contains two electrons. It is also well known that the main stage for pairing is the copper oxide plane. Most models treat pairing to happen independently at each plane as first approximation. The high resistivity along the c-axis infers a high hopping price along that direction. This justifies the treatment of the Cu-O planes as discrete and weakly coupled layers. Different from the superconductivity in metals in which the carrier density is high, the carrier density in Cu-O planes is low whereas T_c is high and the coherence length is very short in HTSC. The coherence length, 10-30Å is almost as short as the distance between a few Cu-O planes. Short coherence length in HTSC means the size of the Cooper pair is small, and the electrons are strongly bound leading to large value for $2\Delta/k_B T_c$ as compared to the BCS superconductors in which the size of the Cooper pairs is large$\left(10^{-4} cm = 10^4 Å\right)$. Thus the biggest puzzle of the cuprates is the mechanism that binds the pairs together such that the coherence length is short.

The phonon-based pairing mechanism that worked for the BCS type superconductors does not seem to be very successful for HTSC. Also there was not a striking isotope effect measurement that could settle the importance of the ion masses involved. This leads to the proposal of other models with different kinds of 'glue' that bind the electron pairs. Because of the proximity to the anti-ferromagnetic regime, it has been proposed that instead of phonons, magnetically mediated interactions could act as the pairing glue. (Scalapino, 1986). A precedent for this kind of mechanism exists in ^3He, where spin fluctuations mediate the pairing that leads to the superfluid state, and similar mechanisms have been proposed for heavy fermions and some materials. It was also proposed (Anderson, 1987) that superconductivity could arise

from the doping of spin $- 1/2$ particle singlets, resulting in quantum fluctuations that would disorder the anti-ferromagnetics (AF) phase, resulting in a liquid of singlet pairs. This provides a close link between the pairing for superconductivity and the magnetism in the sample.

It has also been observed that long-range dipolar interactions provide insight into the properties of the high-temperature superconductors (Norman, 2011 and Levinsen et al, 2015). It is, therefore, assumed that there could exist dipole-dipole interactions, dipole-electron interactions, and thus there could exist inherent electric and magnetic fields that may affect the properties of a superconductor. In what follows such effects have been considered to study the properties of superconductors.

4.2 Effect of the electric field E on the oscillating Cooper pairs that oscillate parallel to the CuO$_2$ planes.

Since the superconducting charge carriers in CuO$_2$ planes flow along theCuO$_2$ planes, the superconducting Cooper pairs may interact with each other as they flow along the CuO$_2$ plane. If the Cooper pairs and positive ions interact with each other it may lead to the creation of an electric field that may act on the Cooper pairs. The net interaction term may be of the form, H_O.

$$H_O = \frac{p^2}{2m} + \frac{1}{2}kx^2 + E\,(2e)\,x \tag{4.1}$$

where $k = m\omega^2$ and x is the distance over which the electric field acts. The first term is the possible potential energy and the second term is the perturbation. For an i-th interacting Cooper pair we can write,

$$H_i = \frac{p_i{}^2}{2m_i} + \frac{1}{2}kx_i{}^2 + E\,(2e)\,x_i \tag{4.2}$$

Where p_i and m_i are momentum and mass of the i-th interacting Cooper pair respectively.

For an assembly of N such interacting Cooper pairs, the total Hamiltonian H can be written as:

$$H = \sum_{i=1}^{N} \left[\frac{p_i^2}{2m_i} + \frac{1}{2} kx_i^2 + E(2e)\, x_i \right]$$

(4.3)

To convert momentum p and the coordinate x into creation $(b^\dagger)$ and annihilation operators (b) of the Cooper pairs. We know that

$$b = \left(\frac{m\omega}{2\hbar}\right)^{1/2}\left(x + i\frac{p}{m\omega}\right)$$

(4.4)

$$b^\dagger = \left(\frac{m\omega}{2\hbar}\right)^{1/2}\left(x - i\frac{p}{m\omega}\right)$$

(4.5)

Adding Eqs. (4.4) and (4.5) we get,

$$(b + b^\dagger) = 2x\left(\frac{m\omega}{2\hbar}\right)^{1/2} = x\left(\frac{2m\omega}{\hbar}\right)^{1/2}$$

or

$$x = \left(\frac{\hbar}{2m\omega}\right)^{1/2}(b + b^\dagger)$$

(4.6)

Subtracting Eqs. (4.4) and (4.5) we get,

$$(b - b^\dagger) = 2i\frac{p}{\omega m}\left(\frac{m\omega}{2\hbar}\right)^{1/2} = i\frac{p}{m}\left(\frac{2m}{\hbar\omega}\right)^{1/2}$$

or

$$p = \frac{m}{i}\left(\frac{\hbar\omega}{2m}\right)^{1/2}(b - b^\dagger) = -i\left(\frac{m\hbar\omega}{2}\right)^{1/2}(b - b^\dagger)$$

(4.7)

Substituting for x and p in to Eq. (4.2) the value of H_i in terms of b and $b^\dagger$ andcalculating each term we get,

$$\frac{p^2}{2m} = \frac{1}{2m}\left(-\frac{m\hbar\omega}{2}\right)(b - b^\dagger)(b - b^\dagger) = -\frac{\hbar\omega}{4}(bb - bb^\dagger - b^\dagger b + b^\dagger b^\dagger)$$

(4.8)

and

$$\frac{1}{2}kx^2 = \frac{1}{2}m\omega^2 x^2 = \frac{1}{2}m\omega^2\left(\frac{\hbar}{2m\omega}\right)(b + b^\dagger)(b + b^\dagger)$$

$$= \frac{1}{4}\hbar\omega(bb + bb^\dagger + b^\dagger b + b^\dagger b^\dagger) \tag{4.9}$$

Adding Eqs. (4.8) and (4.9) we get,

$$H_O = \frac{p^2}{2m} + \frac{1}{2}kx^2$$

$$H_O = -\frac{\hbar\omega}{4}(bb - bb^\dagger - b^\dagger b + b^\dagger b^\dagger) + \frac{\hbar\omega}{4}(bb + bb^\dagger + b^\dagger b + b^\dagger b^\dagger)$$

$$H_O = \frac{1}{2}\hbar\omega(bb^+ + b^+b) \tag{4.10}$$

Eq. (4.10) gives the energy of a harmonic oscillator.

The term $E(2e)x$ refers to the energy added to the Hamiltonian when an electric field is constant over a distance x. whereas the electric field created by dipoles that mediate between the two electrons in a superconductor has to be surmised. We can make an arbitrary guess that such contribution is of the form γx^4 where

$$\gamma = \frac{m\omega^2}{L^2 4\pi^2} \tag{4.11}$$

where L = Length or range of electric field of the dipole.

ω− Angular frequency of the oscillating dipole.

m − Mass of dipole = m_e.

The mass of the dipole should be the reduced mass of the electron and ion since two equal and opposite charges constitute a dipole, negative charge is on the electron and positive on the ion; thus $m = \frac{m_e m_i}{m_e + m_i}$ where m_e and m_i are masses of an electron and an ion, respectively. If $m_e \ll m_i$ then, $m_i \cong \frac{m_e m_i}{m_i} \cong m_e$.

Eq. (4.11) is derived as follows,

Energy= Force x distance=mass x acceleration x distance

$$E=m\frac{L^2}{T^2}=\gamma L^4 \text{ hence } \gamma=\frac{m}{L^2T^2} \tag{4.12}$$

The time period T of oscillation is,

$$T=\frac{1}{f};$$

and

$$\omega=2\pi f$$

or

$$f=\frac{\omega}{2\pi}=\frac{1}{T}$$

or

$$\frac{1}{T^2}=\frac{\omega^2}{4\pi^2} \tag{4.13}$$

Combining Eqs. (4.12) and (4.13) we get,

$$\gamma=\frac{m\omega^2}{L^2 4\pi^2} \text{ which is the result in Eq. (4.11)}$$

However, we multiply γ with 2e since the electric field is created by dipoles mediated between the two electrons,

Therefore, the Hamiltonian of Eq. (4.3) becomes:

$$H=H_O + 2e\gamma x^4 = \frac{P^2}{2m}+\frac{1}{2}m\omega^2 x^2+\frac{2em\omega^2}{4\pi^2 L^2}x^4 \tag{4.14}$$

Using Eqs. (4.6), (4.7), (4.10) Eq.4.14 becomes,

$$H =\frac{1}{2}\hbar\omega(bb^\dagger + bb^\dagger)+\gamma\left[\frac{\hbar^2}{4m^2\omega^2}(b + b^\dagger)^4\right]$$

$$= \frac{1}{2}\hbar\omega(bb^\dagger + bb^\dagger)+\frac{2em\omega^2}{L^2 4\pi^2}\left[\frac{\hbar^2}{4m^2\omega^2}(b + b^\dagger)^4\right]$$

or

$$H = \frac{\hbar\omega}{2}(bb^\dagger + b^\dagger b) + \frac{e\hbar^2}{8\pi^2 mL^2}(bbbb + 4bbbb^\dagger + 6bbb^\dagger b^\dagger$$

$$+ 4bb^\dagger b^\dagger b^\dagger + b^\dagger b^\dagger b^\dagger b^\dagger) \tag{4.15}$$

Using Eq. (4.15), we calculate the expectation value of energy E_n, using $E_n = \langle n|H|n\rangle$ we get,

$$E_n = \langle n|H|n\rangle = \frac{\hbar\omega}{2}\{\langle n|bb^\dagger|n\rangle + \langle n|b^\dagger b|n\rangle\} + \frac{e\hbar^2}{8\pi^2 mL^2}\{\langle n|bbbb|n\rangle + \langle n|4bbbb^\dagger|n\rangle +$$

$$\langle n|6bbb^\dagger b^\dagger|n\rangle + \langle n|4bb^\dagger b^\dagger b^\dagger|n\rangle + \langle n|b^\dagger b^\dagger b^\dagger b^\dagger|n\rangle\} \tag{4.16}$$

On calculating each part of Eq. (4.16), we get,

$$\langle n|bb^\dagger|n\rangle = \langle n|n+1|n\rangle = (n+1)\langle n|n\rangle = (n+1) \tag{4.17}$$

For $\langle n|n\rangle = 1$ (normalization condition)

$$\langle n|bb^\dagger|n\rangle = \langle n|n|n\rangle = n\langle n|n\rangle = n \tag{4.18}$$

For $\langle n|n\rangle = 1$ (normalization condition)

$$\langle n|bbbb|n\rangle = \langle n|n^2|n-4\rangle = n^2\langle n|n-4\rangle = 0 \tag{4.19}$$

For $\langle n|n-1\rangle = 0$ (orthogonality condition)

$$\langle n|4bbbb^\dagger|n\rangle = 4\langle n|(n+1)^{\frac{1}{2}}n^{\frac{3}{2}}|n-3\rangle = 4\{(n+1)^{\frac{1}{2}}n^{\frac{3}{2}}\langle n|n-3\rangle\} = 0 \tag{4.20}$$

for $\langle n|n-1\rangle = 0$ (orthogonality condition)

$$\langle n|6bbb^\dagger b^\dagger|n\rangle = 6\langle n|n(n+1)|n\rangle = 6(n^2+n)\langle n|n\rangle = 6n^2 + 6n \tag{4.21}$$

for $\langle n|n\rangle = 1$ (normalization condition)

$$\langle n|4bb^\dagger b^\dagger b^\dagger|n\rangle = 4\langle n|(n+1)^{\frac{3}{2}}n^{\frac{1}{2}}|n+3\rangle = 4(n+1)^{\frac{1}{2}}n^{\frac{3}{2}}\langle n|n+3\rangle = 0 \quad (4.22)$$

for $\langle n|n-1\rangle = 0$ (orthogonality condition)

$$\langle n|b^\dagger b^\dagger b^\dagger b^\dagger|n\rangle = \langle n|(n+)^2|n+4\rangle = (n+1)^2\langle n|n+4\rangle = 0 \quad (4.23)$$

for $\langle n|n+1\rangle = 0$ (orthogonality condition)

Eq. (4.16) reduces to (4.24) by adding Eqs. (4.17) to (4.23)

$$E_n = \frac{\hbar\omega}{2}\{(n+1)+n\} + \frac{\hbar^2 e}{8m\pi^2 L^2}(6n^2+6n) = \frac{\hbar\omega}{2}(2n+1) + \frac{\hbar^2 e}{8m\pi^2 L^2}(6n^2+6n) \quad (4.24)$$

Eq. (4.24) gives energy excitation spectrum where n=0, 1, 2,…

For $n = 0$, we get the ground state energy E_0,

$$E_o = \frac{\hbar\omega}{2} \quad (4.25)$$

For $n = 1$, we get the next state E_1 above E_0,

$$E_1 = \frac{3\hbar\omega}{2} + \frac{3e\hbar^2}{2m\pi^2 L^2} \quad (4.26)$$

Using Eqs. (4.25) and (4.26) we calculate the energy gap Δ where $\Delta = E_1 - E_O$

$$\Delta = E_1 - E_O = \frac{3\hbar\omega}{2} + \frac{3e\hbar^2}{2m\pi^2 L^2} - \frac{\hbar\omega}{2} = \hbar\omega + \frac{3e\hbar^2}{2m\pi^2 L^2} \quad (4.27)$$

Eq. (4.27) reduces to (4.28) such that,

$$\Delta = E_1 - E_O = \frac{2m\pi^2 \hbar \omega L^2 + 3e\hbar^2}{2m\pi^2 L^2} \qquad (4.28)$$

4.3 Effect of Applied Magnetic Field on a two-dimensional square lattice.

Magnetic flux quantization provides evidence for Cooper pairing thus there exists magnetic flux in a superconducting material, but ofa strength that will not destroy superconductivity. Consequently magnetically mediated interactions could act as the pairing glue. (Scalapino, 1986).
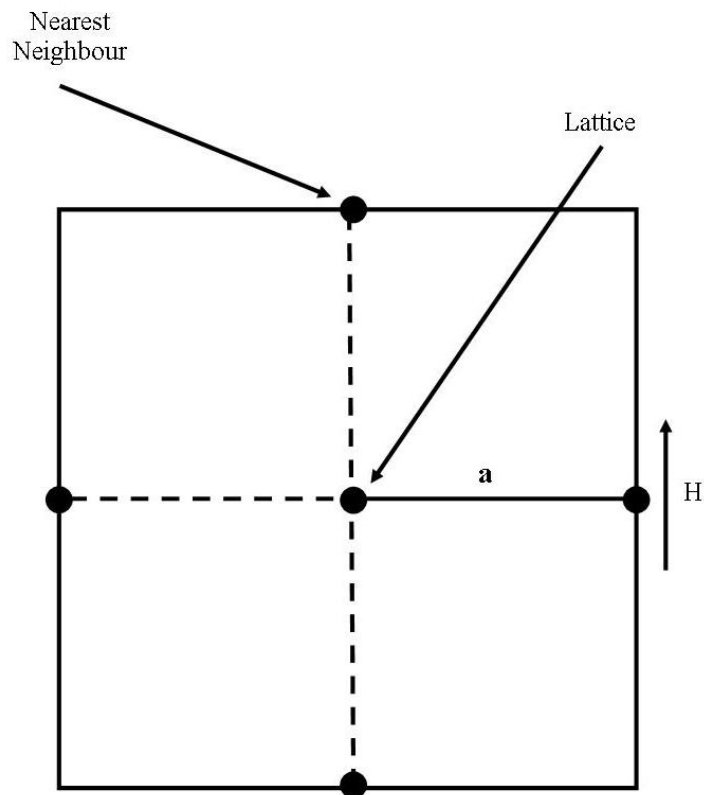

Fig. 4.1. shows application of magnetic field H to 2D square lattice.

Suppose we consider a two-dimensional square lattice of spacing *a,* immersed in a uniform magnetic field,*H*, perpendicular to it as shown in Figure 4.1. Consider an electron with its four immediate neighbors; the electron will undergo two periodic motions.

t – The period of motion of an electron in a state with a crystal momentum.

$$p = \frac{2\pi\hbar}{a} \tag{4.29}$$

Since p. a = h p is momentum, a is lattice spacing where h = $2\pi\hbar$.

If t is the time taken for the electron to travel through a distance a (lattice spacing) say with velocity v, the momentum p of the electron is,

$$p = \frac{2\pi\hbar}{a} = mv$$

OR

$$v = \frac{2\pi\hbar}{ma}$$

then $t = \dfrac{a}{v} = \dfrac{ma^2}{2\pi\hbar}$ $\tag{4.30}$

If τ - is the characteristic period of the electron under uniform applied magnetic field H (time required by an electron to move once on a circular path), H is the uniform magnetic field applied perpendicular to the two dimensional square lattice of spacing a, and if f is the cyclotron frequency such that,

$$f = \frac{eH}{mc}$$

And since T = $\tau = \dfrac{1}{f}$,

$$\tau = \frac{mc}{eH} \tag{4.31}$$

Let the ratio of t to τ be α such that, using Eqs. (4.30) and (4.31) gives,

$$\alpha = \frac{t}{\tau} = \frac{a^2 H}{2\pi\left(\frac{hc}{e}\right)} = \frac{a^2 H}{\Phi_0} = \frac{Flux\ through\ the\ lattice\ cell}{one\ flux\ quantum} \tag{4.32}$$

A subatomic particle such as an electron has particle-like and wave-like properties. For instance, when a particle of mass m moves at speed v, it has energy E = $\dfrac{mv^2}{2}$ and momentum $p = mv$. Such a particle also has wave-like properties, the

wavelength λ being related to the momentum p of the particle by the de Broglie equation.

$$\lambda = \frac{h}{p} \tag{4.33}$$

where h is Planck's constant. From this wave-particle duality, following Heisenberg's uncertainty principle for position x and time t, and energy E and time t are given by

$$\Delta x \Delta p \approx h, \ \Delta E \Delta t \approx h \tag{4.34}$$

where $\Delta \approx k_B T_c$ because Cooper pairs break up at T_c and E is energy, p is momentum and h is Planck's constant. Let us consider the formation of a Cooper pair bearing in mind the uncertainty principle given by Eq. (4.34).

Assuming that the scale of time to establish Cooper pair is given by,

$$t \approx \frac{h}{\Delta} = \frac{h}{k_B T_c} \tag{4.35}$$

superconductivity cannot be observed if the time is shorter than t. t is the time taken to establish a Cooper pair and Cooper pairs break up at T_c. Distance ξ by which the electron moves to form the pair is the *Pippard coherence length* (Pippard, 1953), given by,

$$\xi = t v_F \tag{4.36}$$

where v_F is the Fermi velocity. The time t can also be assumed to be the time taken by an electron to move through the lattice of size a with velocity v given by,

$$t = \frac{a}{v} \tag{4.37}$$

For the case of applied uniform magnetic field H on a 2-D square lattice, Eq. (4.37) reduces to

$$t = a^2 H \tag{4.38}$$

Combining Eqs. (4.32) and (4.37)

where a^2H is the flux through the lattice cell. Equating Eqs. (4.35) and (4.38), we get

$$a^2H = \frac{h}{k_B T_c}$$

or

$$a = \sqrt{\frac{h}{k_B T_c H}} \tag{4.39}$$

Eq. (4.39) gives T_c, such that,

$$T_c = \frac{h}{a^2 H k_B} \tag{4.40}$$

Equations (4.32), (4.39) and (4.40) were used in studying thermodynamic properties of HTSC systems under influence of applied external magnetic field H.

4.4 Effect of effective magnetic flux per plaquette

Consider the Harper's equation (Hofstadter, 1976)

$$\frac{\epsilon+4}{\gamma}F(x) = x^2 F(x) - F''(x) - \frac{\gamma}{12}[F''''(x) + x^4 F(x)] \text{ where } x = n\gamma^{\frac{1}{2}}, \gamma = 2\pi\Phi$$

Φ = Effective magnetic flux per plaquette, x = electronic density, ϵ is energy corresponding to one particle spectrum.

Then

$$\epsilon F(x) = -4F(x) + \gamma x^2 F(x) - \gamma F''(x) - \frac{\gamma^2}{12}[F''''(x) + x^4 F(x)] \tag{4.41}$$

The unperturbed part of Harper's equation is,

$$x^2 F(x) - F''(x) = (2a^{\dagger}a + 1)\, F(x) \tag{4.42}$$

substituting Eq. (4.42) into (4.41) we get,

$$\epsilon = -4F(x) + \gamma(2a^{\dagger}a + 1)\, F(x) - \frac{\gamma^2}{12}[F''''(x) + x^4 F(x)] \tag{4.43}$$

$$\epsilon = -4F(x) + \gamma(2a^\dagger a + 1) F(x) - \frac{\gamma^2}{12}\left[\frac{d^4}{dx^4}F(x) + x^4 F(x)\right] \tag{4.44}$$

On calculating the expectation value of Eq. (4.44),

$$\langle F(x)|\epsilon|F(x)\rangle = -4\langle F(x)|F(x)\rangle + \gamma(2a^\dagger a + 1)\langle F(x)|F(x)\rangle - \frac{\gamma^2}{12}\left\langle F(x)\left|\frac{d^4}{dx^4} + x^4\right|F(x)\right\rangle$$

or

$$E_n = -4 + \gamma (2n + 1) - \frac{\gamma^2}{12}\langle F_n\left|\frac{d^4}{dx^4} + x^4\right|F_n\rangle \tag{4.45}$$

where $\langle F(x)|F(x)\rangle = 1$ due to normalization and $a^\dagger a = $n.

From Eq. (4.45) $\left(\frac{d^4}{dx^4} + x^4\right)$ is the perturbing term. To calculate the perturbation term,

we substitute for x and $\frac{d}{dx}$ which are $x = \frac{1}{\sqrt{2}} (a + a^\dagger)$ and $\frac{d}{dx} = \frac{1}{\sqrt{2}} (a - a^\dagger)$ in Eq. (4.45)

to get,

$$\frac{d^4}{dx^4} + x^4 = \left[\frac{1}{\sqrt{2}}(a - a^\dagger)\right]^4 + \left[\frac{1}{\sqrt{2}}(a + a^\dagger)\right]^4$$

$$= \frac{1}{2}[(a^\dagger)^4 + aaa^\dagger a^\dagger + aa^\dagger aa^\dagger + a^\dagger aaa^\dagger + aa^\dagger a^\dagger a + a^\dagger aa^\dagger a + a^\dagger a^\dagger aa] \tag{4.46}$$

Combining Eqs. (4.45) and (4.46) and using quantities in (4.46) we get,

$$a^\dagger |F_n\rangle = (n + 1)^{\frac{1}{2}} |F_{n+1}\rangle \text{ And } a|F_n\rangle = n^{\frac{1}{2}} |F_{n-1}\rangle \tag{4.47}$$

The expectation value of Eq. (4.45) becomes,

$$\langle F_n\left|\frac{d^4}{dx^4} + x^4\right|F_n\rangle = \frac{1}{2}\left[(n + 1)(n + 2)(n + 1)^2 + \left(n(n + 1)\right)^2 + n^2 + \right.$$

$$\left. n(n - 1)\right] = \frac{3}{4}[(2n + 1)^2 + 1] \tag{4.48}$$

Substituting Eqs. (4.48) into (4.47) we get,

$$E_n = -4 + \gamma (2n + 1) - \frac{\gamma^2}{16}[(2n + 1)^2 + 1] \tag{4.49}$$

At the temperatures that are of interest, it is necessary to consider the energy

difference between states in which hopping electron is on one site and then when it is

on another site of similar symmetry. The difference in energy levels of the two sites gives the probability amplitude Green's function, which, according to Quantum treatment of lattice vibrations is equivalent to the thermal activation factor $e^{-\frac{\Delta E}{kT}}$. We now multiply Eq. (4.49) with the thermal activation factor and this gives, say E, such that,

$$E = \left[-4 + \gamma(2n + 1) - \frac{\gamma^2}{16}\{(2n+1)^2 + 1\}\right]e^{-\frac{\Delta \epsilon}{kT}} \tag{4.50}$$

The specific heat $C_v = \left(\frac{\partial E}{\partial T}\right)$

$$= \frac{\partial\left(-4 + \gamma(2n+1) - \frac{\gamma^2}{16}[(2n+1)^2+1]e^{-\frac{\Delta\epsilon}{kT}}\right)}{\partial T} = -\frac{\gamma^2}{16}[(2n+1)^2 + 1]\left(\frac{\Delta\epsilon}{k}\right)\left(-\frac{1}{T^2}\right)e^{-\frac{\Delta\epsilon}{kT}} \tag{4.51}$$

To determine the transition temperature and entropy, Equations

$\left(\frac{\partial C_v}{\partial T}\right)_{T=T_c} = 0$ and $S = \int \frac{C_v dT}{T}$ were used.

To calculate T_c, we write,

$$\frac{\partial C_v}{\partial T} = -\frac{\gamma^2}{16}[(2n+1)^2 + 1]\left(\frac{\Delta\epsilon}{k}\right)\left(\frac{-2}{T^3}\right)e^{-\frac{\Delta\epsilon}{kT}} + \frac{\gamma^2}{16T^2}[(2n+1)^2 + 1]\left(-\frac{\Delta\epsilon}{k}\right)\left(-\frac{1}{T^2}\right)e^{-\frac{\Delta\epsilon}{kT}}$$

or

$$= \frac{\gamma^2}{8T^3}[(2n+1)^2 + 1]e^{-\frac{\Delta\epsilon}{kT}} - \frac{\gamma^2}{16T^4}[(2n+1)^2 + 1]\left(-\frac{\Delta\epsilon}{k}\right)^2 e^{-\frac{\Delta\epsilon}{kT}}$$

At T_c, $\left(\frac{\partial C_v}{\partial T}\right) = 0$,

$$\left(\frac{\partial C_v}{\partial T}\right)_{T=T_c} = \frac{\gamma^2}{8T_c^3}[(2n+1)^2 + 1]e^{-\frac{\Delta\epsilon}{kT_c}} - \frac{\gamma^2}{16T_c^4}[(2n+1)^2 + 1]\left(-\frac{\Delta\epsilon}{k}\right)^2 e^{-\frac{\Delta\epsilon}{kT_c}} = 0$$

$$2 - \frac{\Delta\epsilon}{T_c} = 0$$

or

$$T_c = \frac{\Delta\epsilon}{2} \tag{4.52}$$

The value of $\Delta\epsilon$ can be obtained from Eq. (4.49) where $\Delta\epsilon=E_o - E_1$

For n=0,

$$E_0 = -4 + \gamma - \frac{\gamma^2}{8} \tag{4.53}$$

and for n=1,

$$E_1 = -4 + 3\gamma - \frac{5\gamma^2}{8} \tag{4.54}$$

Subtracting Eq. (4.53) from Eq. (4.54), we get, $\Delta\epsilon$ as,

$$\Delta\epsilon = E_o - E_1 = -4 + \gamma - \frac{\gamma^2}{8} + 4 + 3\gamma + \frac{5\gamma^2}{8} = \frac{\gamma^2}{2} - 2\gamma \tag{4.55}$$

for $\gamma = 2\pi\Phi$ hence

$$\Delta\epsilon = \gamma\left(\frac{\gamma}{2} - 2\right)$$

or

$$2\pi\Phi\left(\frac{2\pi\Phi}{2} - 2\right) = 2\pi^2\Phi^2 - 4\pi\Phi$$

and thus

$$T_c = \frac{\Delta\epsilon}{2} = \pi^2\Phi^2 - 2\pi\Phi \tag{4.56}$$

Eq. (4.56) becomes,

$$\pi^2\Phi^2 - 2\pi\Phi - T_c = 0 \tag{4.57}$$

Substituting for π in Eq. (4.57) becomes,

$$9.87\Phi^2 - 6.28\Phi - T_c = 0 \tag{4.58}$$

Which is a quadratic equation of the form $ax^2 + bx + c = 0$, and can be used to obtain

Φ in terms of T_c.

Thus,

$$\Phi = \frac{-b \pm \sqrt{b^2 - 4ac}}{2a} \text{ where a} = 9.87, \text{ b} = -6.28 \text{ and c} = -T_c$$

or

$$\Phi = \frac{6.28 \pm \sqrt{39.44 + 39.48 T_c}}{19.74} \qquad (4.59)$$

Eq. (4.59) is used in studying the magnetic flux per plaquette for any given value of T_c of some HTSC systems.

CHAPTER FIVE

RESULTS AND DISCUSSIONS

5.1   Introduction

The chapter presents the results obtained for field dependence of the properties of high temperatures superconductors. The results presented were for determination of the energy gap (Δ) of a YBCO system due to an electric field E created by oscillating Cooper Pairs along the CuO planes and its effect on the transition temperature T_c, the determination of transition temperature T_c of BSCCO and YBCO systems when an external magnetic field H is applied on them, and the investigation of the effect of applied magnetic flux (Φ) on transition temperature T_c on various high temperature superconductors.

5.2   Determination of Energy Gap (Δ) of a YBCO system.

To determine the value of Enegy Gap (Δ) in Eq. (4.28), the following parameters are used. $\hbar\omega$=0.08eV for a YBCO system (Alexandrov et al., 2012), $\hbar = 1.055 \times 10^{-34}$Js, $\omega = 1.0 \times 10^{14}$rad/s, e = 1.6 x 10^{-19}C and L = 1.0 x 10^{-6}m the value of Δ turns out to be, Δ = 62.5meV which is three times the experimental value of 20meV (Tsai et al, 1989). By taking $\rho = 2\Delta/k_B T_c$ for Δ=62.5meV and ρ=5 and 8, the value of T_c turns out to lie between 289.86K and 181.16K, respectively. However, for experimental value of ρ=6 (Tsai et al, 1989), the value of $T_c \cong 240$K.

5.3   Graphical Analysis of Superconducting Parameter and Temperature

Variation of Superconducting Parameter $\rho(2\Delta/k_BT_c)$ WithT_c

Using experimental values of superconducting parameter $\rho = 5 - 8$ and

$\Delta = 20\text{meV}$ for a YBCO system graph was drawn for variation of ρ against T_c. The

superconducting parameter $\rho$was found to vary with temperature of the system as

shown in the graph in Fig. 5.1.

Using experimental values of superconducting parameter $\rho = 5 - 8$ and

calculated value of $\Delta = 62.5\text{meV}$ for a YBCO system. The superconducting

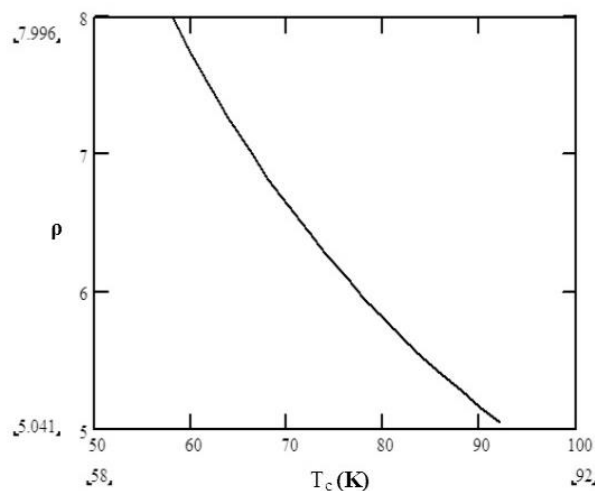parameter ρ is found to vary with temperature of the system as shown in the graph in

Fig. 5.2.

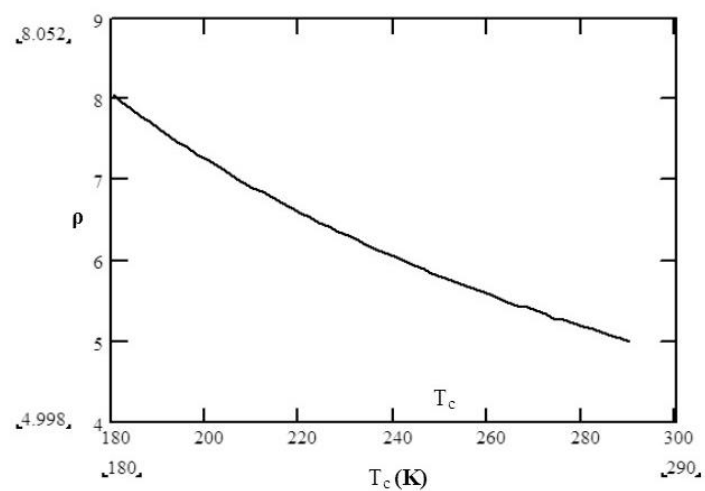

Fig. 5.1. Variation of ρ with T$_c$ for Δ = 20meV   Fig. 5.2. Variation of ρ with T$_c$ for Δ = 62.5meV

There is non-linear increase in the values of T_c with a decrease in the values

of$\rho$when$\Delta = 20\text{meV}$ for $YBa_2Cu_3O_{7-\delta}$, and $\Delta = 62.5\text{meV}$ is for a YBCO system due

to an electric field created by oscillating Cooper pairs along the CuO_2 planes.The

graphs in Figures 5.1 and 5.2 are similar in shape for experimental value of

Δ = 20meV and calculated value of Δ = 62.5meV. The values of T_c lie between 58

and 92K for Δ = 20meV.The values of T_c lie between and 181.16K and 289.86K for

Δ = 62.5meV. For typical experimental value of ρ = 6 (Tsai et al, 1989), the value of

T_c turns out to be 77K when Δ = 20meV and$T_c \cong$ 240K for Δ = 62.5meV. The

calculated value of the energy gap of a YBCO system is three times the experimental

value and this leads to increase in the value of T_c.

5.4   Variation of αWith Lattice Constant a

By taking H_{c_1}= 100G - H_{c_2}=3.0 x 10^6G for YBaCuO and BiSrCaCuO systems

(Batlogg B, 1994), a = 1-3Å (Uchida, 1997) for a system $\hbar$ = 1.055 x 10^{-34}Js,

c = 3.0 x 10^8m/s and e = 1.6 x 10^{-19}C, then Eq. (4.32) is used for calculating

different values of the ratio of the flux through the lattice cell to one flux quantum (or

ratio of the time taken by the electron to move through the lattice of size, a, to the

characteristic time of an electron in a magnetic field/time to move once on a circular

path)Figures5.3, 5.4, 5.5 and 5.6 show the variation of α with lattice constant for

different values of H.
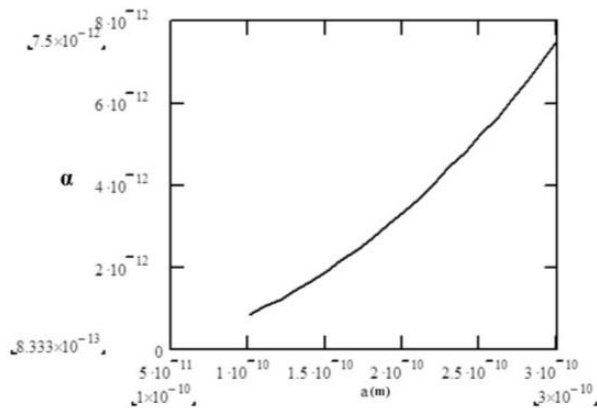
Fig. 5.3. Variation of α with *a* for H = 100G
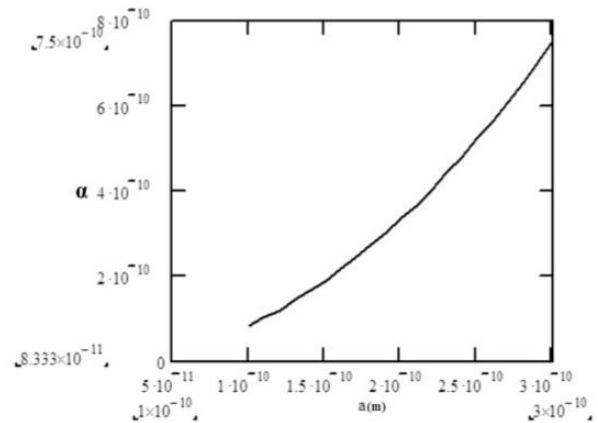
Fig. 5.4. Variation of α with *a* for H = 10000G
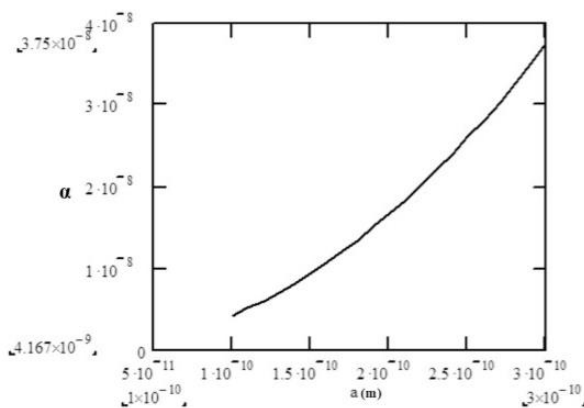
Fig. 5.5. Variation of α with *a* for H = 500000G
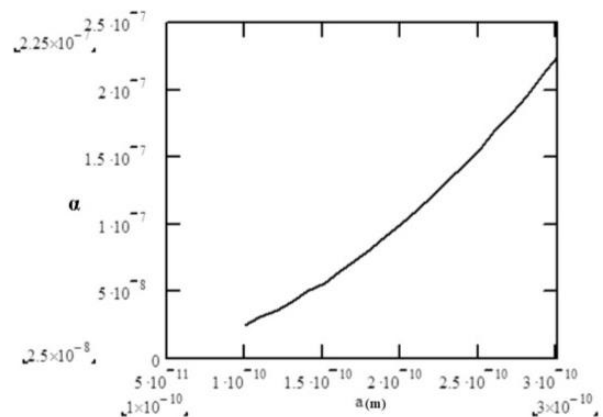
Fig. 5.6. Variation of α with *a* for H = 3000000G

For $H = 100G$, the values of α lies between 8.33 x 10^{-13} and 7.5 x 10^{-12} when $a = 1\text{Å}$ and when $a = 3\text{Å}$ respectively. For $H = 10000G$, the values of α lies between 8.33 x 10^{-11} and 7.5 x 10^{-10} when $a = 1\text{Å}$ and when $a = 3\text{Å}$ respectively. For $H = 500000G$, the values of α lies between 4.12 x 10^{-9} and 3.75 x 10^{-8} when $a = 1\text{Å}$ and when $a = 3\text{Å}$, respectively. For $H = 3000000G$, the values of α lies between 2.5 x 10^{-8} and 2.25 x 10^{-7} when $a = 1\text{Å}$ and when $a = 3\text{Å}$ respectively.

Figures 5.3 to 5.6show that the value of α increases with increase in applied magnetic field H. When the superconductor changes from mixed/vortex state to normal state (Cooper pairs break up), the value of α is 2.25 x 10^{-7} whenH_{c_2} = $3000000G$ and $a = 3Å$.

5.5 Determination of T_c for BiSrCaCuO and YBaCuOSystems when Placed in an External Magnetic Field.

Equation (4.40) was used in calculating the transition temperature at which a superconductor changes from superconducting state to normal state and vice versa. To get the value of T_c from Eq. (4.40), the following parameters were used. H_{c_2} = 3 x10^6G for BiSrCaCuO/YBaCuO systems (Batlogg B, 1994), $h = 6.63$ x 10^{-34}Js, $a = 3$ x $10^{-10}m$ (Uchida, 1997) and k_B = 1.38 x$10^{-23}J/K$.The value of T_c turns out to beT_c = $177K$.

To get the value of a (lattice parameter/spacing), for T_c = $300K$ (room temperature) and H_{c_2} = 3 x10^6G for BiSrCaCuO/YBaCuO systems. Eq. (4.39) is used and the value of a turns out to be a = $2.3Å$.

5.6 Variation of a With T_c

Substituting experimental valuesH_{c_2} = 3 x10^6G for BiSrCaCuO/YBaCuO systems (Batlogg B, 1994), $h = 6.63$ x 10^{-34}JS and k_B = 1.38 x$10^{-23}J/K$ into Eq. (4.39), the lattice constant of the system was found to vary with the transition temperature of the system as shown in the graph in Figure 5.7.
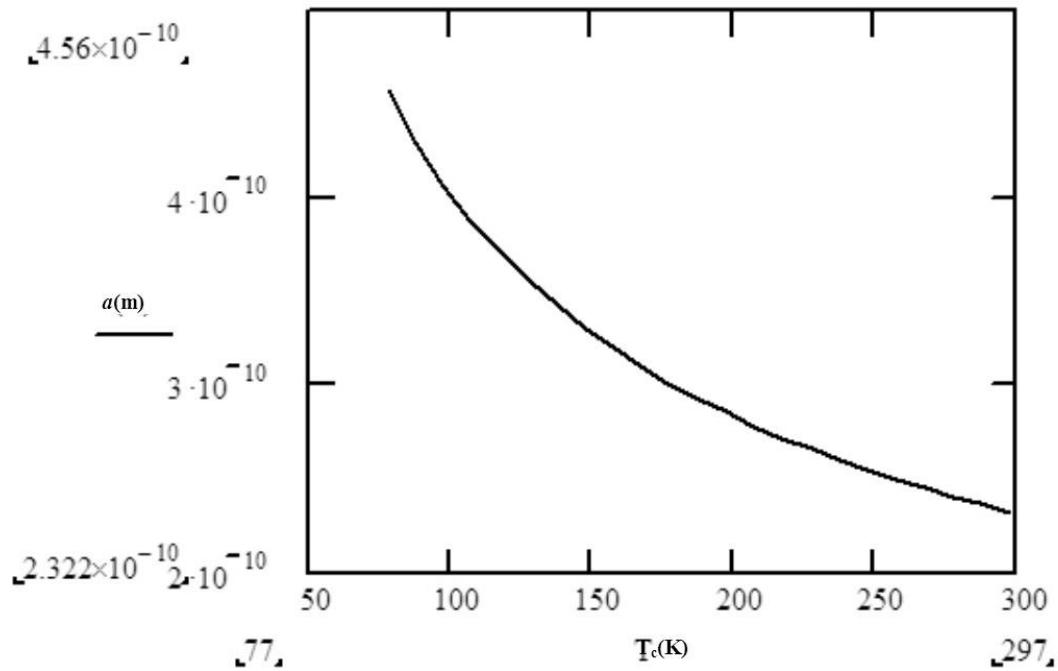
Fig. 5.7. Plot of Variation of a with T_c for H = 3000000G

There is a non-linear decrease in the value of a with increase in T_c when applied magnetic field is considered. From the graph the value of T_c turns out to be $177K$ when $H = 3$ x 10^6G for BSSCO and YBCO systems which is almost double the experimental value of $T_c = 95K$ (Batlogg, 1994).

5.7   Variation of Magnetic Flux(Φ) With T_c

Substituting experimental values for T_c between 77K and 300Kinto Eq. (4.59), the magnetic flux per plaquette was found to vary with the increase in the transition temperature of the system as shown in the graph in Figure 5.8
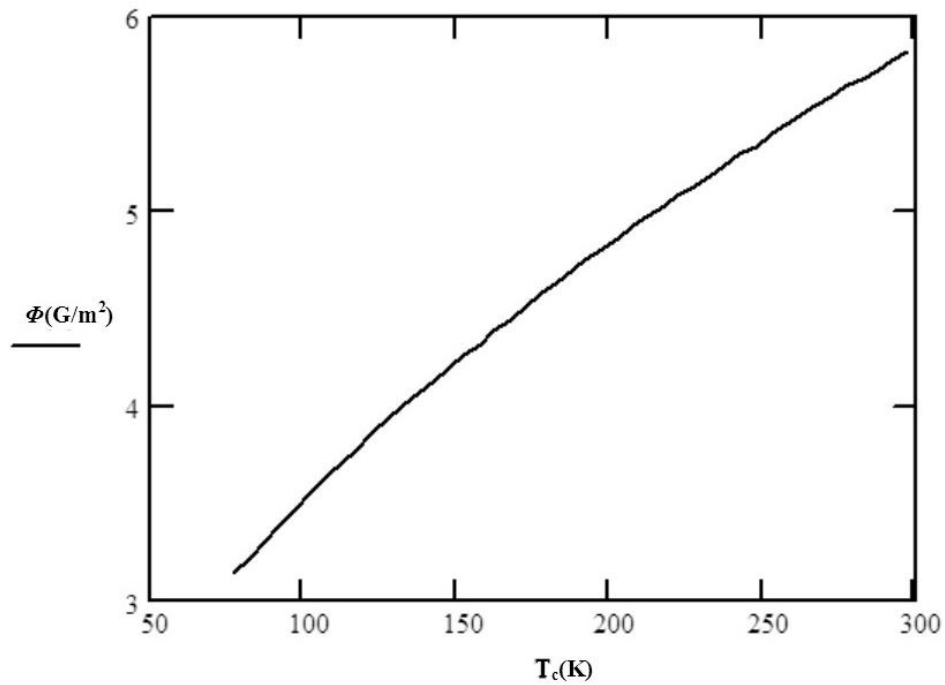
Fig. 5.8. Variation of Φ with T$_c$

In figure5.8, there was a non-linear increase in the applied magnetic flux Φ with an increase in the transition temperatureT_c. The value of Φ increases with the transition temperature T_c . The value of Φ turns out to be 5.84 G/m^2 when $T_c = 300K$.

5.8   Numerical Evaluation of the Values of Φ for Different HTSC Systems.

By taking different values of T_c between $77K$ and $300K$ for HTSC systems, Eq. (4.59) is used in calculating the value of Φ as in table 5.1below.

Table 5.1 shows calculated values of Φ for Different HTSC Systems.

Superconductor	T_c (K)	Φ (G/m^2)
Y – 123	85	3.27
Tl – 2230	86	3.29
Tl – 2223	114	3.73
Hg - 1123	132	3.99

CHAPTER SIX

CONCLUSIONS AND RECOMMENDATIONS

6.1 Conclusion

Field dependence properties of HTSCs have been studied. It is believed that conductivity in HTSCs takes place along the CuO_2 planes and due to this the oscillating Cooper pairs may interact with each other. If the Cooper pairs and positive ions also interact with each other, they may lead to creation of an electric field which may in turn act on the Cooper pairs. The created electric field E, acts as the perturbation in the Hamiltonian describing the interaction. The study uses second quantization formalism to calculate the expectation value of energy, $(E_n = \langle n|H|n \rangle)$ and the energy gap Δ= 62.5meV for a YBCO system. The value of the energy gap lies in the experimental range of 20meV to 100meV.

The variation of superconducting parameter ρ $(2\Delta/k_B T_c)$ with transition temperature T_c is similar in nature to graphs obtained for different values of different materials which confirms correctness of the calculations(Figures 5.1 and 5.2). The calculations give the highest value of $T_c \cong 289K$ in the range of $181K - 289K$, for ρ values of $5 - 8$. The highest value of $T_c \cong 289K$ is close to the room temperature $T \cong 300K$. Thus if a material with such characteristics can be build or developed, it can have a T_c value close to the room temperature.

The effect of applied magnetic field on a 2-D square lattice has been studied. An electron with its four immediate neighbours undergoes two periodic motions (the period of motion of an electron in a state with a crystal and the characteristic period of the electron under uniform applied magnetic field H). The periodic motion of an

electron in state with crystal momentum p and the periodic time taken by an electron to travel through lattice spacing a. The ratio α of the two periodic motions is equal to the ratio of flux through the lattice cell to one flux quantum. The study established that there is no Meissner expulsion of flux as H increases through the lattice cell. The value of T_c at which a superconductor changes from superconducting state to normal state and vice versa was found to be 177K for BSCCO and YBCO systems at $H_{c_2} = 3.0$ x 10^6G, and the value of α is 2.28 x 10^{-7} when $H_{c_2} = 3.0$ x 10^6G and $a = 3$Å. Also the value of a (lattice constant) at $T_c = 300$K (room temperature) was found to be 2.3Å which is within the experimental range of 1-3Å. Thus a superconductor with lattice constant 2.3Å can be manufactured such that $T_c = 300$K and $H_{c_2} = 3.0$ x 10^6G and it is a very important result.

The effect of effective magnetic flux per plaquette has also been studied where Harper's equation is subject to second quantization formalism and finally established that there is a linear dependence between the values of T_c and effective magnetic flux per plaquette for HTSCs. The value of Φ is 5.84G/m^2 at room temperature (300K) and lies between 3.12-5.84G/m^2 for temperature range of 77-300K.

6.2   Recommendations

The study of applied magnetic field along a-b planes or CuO_2 planes in a 2-D square lattice can be studied in future and its effect on pairing mechanism established.

We could also study linear response to a magnetic field applied perpendicular to the layer by assuming that the field has an orbital coupling to the superconducting order (Hayward et al, 2014) in $YBa_2Cu_3O_{6+x}$ superconductor.

Quantum oscillations due to the dipole electric field and the applied magnetic field could be studied for high-T_c superconductors (Banerjee et al, 2013). Magnetic field enhanced spin freezing on the verge of charge ordering in $YBa_2Cu_3O_{6.45}$ could be studied (Wu et al, 2013). Calculations can also be done to explore the momentum dependent charge correlations in $YBa_2Cu_3O_{6+\delta}$ (Blanco-Canosa, et al, 2013).

It is possible that different combinations of Coulomb interactions can be used to study the properties of heavy-fermion superconductors (Keisuke, et al, 2015). We can study the effect of motion of electrons like a fluid on the properties of a superconductor (Stajic, 2016).

REFERENCES.

Abrikosov, A. A. (1957). Magnetic properties of superconductors of the second group. *SOV. Phys. JETP (Engl.Transl); (United States),5*(6).

Alexandrov, A. S.,& Mott, N. F. (1994). Bipolarons. *Reports on Progress in Physics, 57*(12), 1197.

Alexandrov, A. S.(1999).Comment on Experimental and Theoretical constraints of Bipolaronic superconductivity in high T_c materials: An Impossibility. *Physical reviewletters,82*(12), 2620.

Alexandrov, A. S., (2004). *Proc. Int. Conf. on Basic Problem of HTSC,*(Moscow, 18-22,October)

Alexandrov, A. S., Samson, S. H., & Sica, G. (2012). High- Temperature Superconductivity from Realistic Coulomb and Frolich Interactions.*EPL, (Europhysics Letters), 100* (1), 17011.

Anderson, P. W. (1987). The resonating valence bond state in La2CuO4 and superconductivity.

Andreev, A. F., (1964). Thermal conductivity of the intermediate state of superconductors.*Zh. Eksperim.i Teor. Fiz.,*46.

Arbman, G., & Jarborg, T. (1978). Trend studies of A15 compounds by self consistent band calculations. *Solid State Communications, 26*(11)**,** 857-861.

Ashkin, M., Gavaler, J. R., Greggi, J., & Decroux, M. (1984). The upper critical field of NbN films II. *Journal of Applied Physics, 55*(4), 1044-1048.

Bardeen, J., Cooper, L. N., and Schriffer, R. (1957). Theory of superconductivity. *Physics Review, 108*(5),1175.

Bardeen, J., (1962). *Phys. Rev. Lett.* **1**,251.

Batlogg, B. (1994). Physical properties of high- T_c superconductors. *Aalam Al-Zarra*, 30-40.

Banerjee, S., Zhang, S., & Randeria, M. (2013). Theory of quantum oscillations in the vortex-liquid state of high-T_c superconductors. *Nature Communications,* 4, 1700.

Bednorz, J. G., & Muller, K. A. (1986). Possible high-T_c superconductivity in the Ba-La-Cu-O system. In *Ten years of superconductivity*: 1980-1990 (pp. 267-271). Springer Netherlands.

Blanco-Canosa, S., Frano, A., Leow, T., Lu, Y., Porras, J., Ghirighelli, G., & Weschke, E., B. (2013). Momentum dependant charge correlations in YBa2Cu3O6+δ superconductors probed by resonant X-ray scattering: evidence for three competing phases. *Physical review Letters, 110*(18), 187001.

Blatter, G., Geshkenbein, V. B., & Larkin, A. I. (1992). From isotropic to anisotropic superconductors: a scaling approach. *Physical Review Letters,68*(6), 875.

Bhattacharya, R. N.,& Paranthaman, M.P. (2011). High Temperature Superconductors. *John Willey& Sons-VCH*, pp 8.

Boekholt, M., Hoffman, M., and Guntherodt, G., (1991). Detection of an anisotropy

of the superconducting gap in $Bi_2Sr_2CaCu_2O_{8+\delta}$ Single Crystal by Roman and tunneling spectroscopy. *Physica C,*175: 127 − 134.

Brizhik, L. S.,& Davydov, A. S. (1984). Nonlinear theory of conductivity in one-dimensional molecular crystals. *Low Temperature Physics, 10* (4), 358-366.

Buckel, W., and Kleiner, R. (2004). Superconductivity: Fundamentals and Applications, a textbook. *John Willey & Sons-VCH*.

Bud'ko, S. L., Lapertot, G., Petrovic, C., Cunningham, C. E., Anderson, N., &Canfield, P. C. (2001). Boron isotope effect in superconducting MgB2. *Physical Review Letters*, *86*(9), 1877 – 1880.

Cava, R. J., Batlogg, B., Krajewski, J. J., Farrow, R., Rupp, L. W., White A. E., Short,K., Peck, W. F., & Kometani, T. (1988). Superconductivity near 30K without copper: The BaO.6KO.4BiO3 Perovskite. *Nature, 332* (6167), 814-816.

Chakraverty, B. K., Ranninger, J., & Feinberg, D. (1998). Experimental and Theoretical Constraints of Bipolaronic Superconductivity in High T_c Materials: An Impossibility. *Physical Review Letters, 81* (2), 433.

Chu, C. W.,Gao, L., Chen, F., Huang, Z. J., Meng, R. L., & Xue, Y. Y. (1993).Superconductivity above 150K in $HgBa_2Ca_2Cu_3O_{8+\delta}$ at high pressure. *Nature*, 365: 323– 325.

Chu, C. W., et al. (2007). *Nature*, 2684–2686.

Chu, C. W., Hor, P. H., Meng, R. L., Gao, L., & Huang, Z. J. (1987). Superconductivity at 52.5K in the La-Ba-Cu-O system. *Science, 235*(4788), 567-569.

Collings, E. W. (1986). Superconductivity, Metallurgy, and Physics ofTitanium Alloys. *Vol. 2:* Applications.

Cronstrom, C., & Noga, M. I. (2001).Third-order phase transition and superconductivity in thin films. *Czechoslovak Journal of Physics, 51* (2), 175-184.

Cui, H.Y. (2002). Cond-mat/0209269.

Davydov, A. S. (1988). Solitons in Molecular Systems (Naukova Dumka, Kiev, 1988),Russian.

Davydov, A. S. (1990). Theoretical investigation of high-temperature superconductivity. *Physics Reports*, *190*(4-5),191-306.

Davydov, A. S. (1991). The lifetime of molecular (Davydov) Solitons. *Journal of Biological Physics, 18* (2), 111-125.

Eliashberg, G. M. (1961). Temperature Green's function for electrons in a superconductor *SOV.Phys-JETP,*12, 1000.

Emery, V. J., & Kivelson, S. A. (1995). Importance of phase fluctuations in superconductors with small superfluid density.*Nature,374* (6521), 434-437.

Emery, V. J., Kivelson, S. A., & Zachar, O. (1997). Spin-gap proximity effect mechanism of high-temperature superconductivity. *Physical Review B*,*56*(10), 6120.

Farrell, D. E., Beck, R. G., Booths M. F., Allen, C. J., Bukowski, E. D., & Ginsberg,D. M. (1990). Superconducting effective – mass anisotropy in $Ti_2Ba_2CaCu_2O_x$. *Physical Review B*, 42(10), 6758.

Frolich, H. (1950). Theory of superconducting state I. The ground state at the absolute zero of temperature. *Physical Review*, *79* (5), 845.

Gammel, P. L., Bishop, D. J., Dolan, G. J., Kwo, J. R., Murray, C. A., Scheemeyer, L.F., & Waszczak, J. V. (1987). Observation of hexagonally correlated flux quanta in$YBa_2Cu_3O_7$. *Physical review Letters, 59* (22), 2592.

Ganin, A. Y., Takayabashi, Y., Khimyak, Y. Z., Margadonna, S., Tamai, A.,Rosseinky, M.J., & Prassides, K. (2008). Bulk superconductivity at 38K in a molecular system. *Nature Materials, 7* (5)**,** 367-371.

Gao, L., Xue, Y. Y., Chen, F., Xiong, Q., Meng, R. L., Ramirez, D., Chu, C. W., Eggert, J. H., & Mao, H. K. (1994). Superconductivity upto 164K in $HgBa2Cm - 1CumOm+2+\delta$ (m=1, 2 and 3) under quasi hydrostatic pressures. *Physical Review B, 50*,4260.

Ginzburg, V. L., & Landau, L. D. (1950). On the theory of superconductivity. *Zh.Eksp.Teor.Fiz;* 20, 1064.

Gorter C. J., & Casimir, H. (1935). On superconductivity I. *In Archives du muse Teyler (pp. 1-15).* Springer Netherlands.

Greenwood, N.N., & Earnshaw, A. (1997). *Chemistry of the elements 2nd Edition.* Butterworth-Heinemann.

Ginzburg, V. and Landau, L. (1950). *Zh. Eksp. Teor. Fiz,***32**, 1442.

Ginzburg, V. L. (2000). *Supercond.* $13, 665 - 677$.

Gor'kov, L. P. & Sokol, A. V. (1987). Phase stratification of an electron liquid in the new superconductors. *ZhETF Pisma Redaktshu,* 46, 333.

Gough, C. E., Colclough, M. S., Forgan,E. M., Jordan, R. G., Keene, M., Muirhead, C.M., Rae, M., Thomas, N., Abell, J.S., & Sutton, S., (1987). Flux quantization in a high T_c-superconductor. *Nature*, $362, 855 - 857$.

Hardy, W. N., Bonn, D. A., Morgan, D. C., Liang, R., & Zhang, K. (1993). Precision measurement of the temperature dependence of λ in $YBa_2Cu_3O_{6.95}$: strongevidence of nodes in the gap function. *Physical Review Letters, 70* (25), $3999 - 4002$.

Hayward, L. E., Hawthorn, D. G., Melko Roger, G. & Sachdev, S. (2014). Angular fluctuations of multi component order describe pseudo gap $YBa_2Cu_3O_{6+x}$. *Science, 343* (6177), 1336-1339.

Hazen, R. M., Finger, L. W., Angel, R. J., Prewitt, C. T., Ross, N. L., Mao, H. K., & Chu, C. W. (1987). Crystallographic description of phases in Y-Ba-Cu-O superconductor. *Physical Review B, 35* (13), 7238.

Hazen, R. M., Finger, L. W., Angel, R. J., Prewitt, C. T., Ross, N. L., Hadidiacos, P. J., & Hermann, A. M. (1987). 100-K superconducting phases in the Tl-Ca-Ba-Cu-O system. *Physical review letters, 60* (16),1657.

Hebard, A. F., Rosseinky, M. J., Haddon, R. C., Murphy, D. W., Glarum, S. H., Pasltra, T.T. M., Ramirez, A. P., & Kortan, A. R. (1991). Potassium-doped C60. *Nature, 350*, 600-601.

Hinks, D. G., Clause, H., & Jorgensen, J. D. (2001). The complex nature of superconductivity in MgB2 as revealed by the reduced total isotope effect. *Nature, 411* (6836), 457 – 460.

Hofstadter, D. R. (1976). Energy levels and wave functions of Bloch electrons in rational and irrational magnetic fields. *Physical review B*, *14* (6), 2239.

Homes, C. C., Dordevic, S. V.,Strongin, M., Bonn, D. A., Liang, R., Hardy, W. N., & Zhao, X. (2004). Universal scaling relation in high-temperature superconductors. *Nature, 430* (6999), 539-541.

Honma, T. & Hor, P. H. (2006). Universal optimal hole-doping concentration in single-layer high-temperature cuprate superconductors. *Superconductor Science and Technology; 19* (9), 907.

Houghton, A., Pelcovits, R. A., & Sudbo, A. (1989). Flux lattice melting in high-T_c superconductors. *Physical Review B,40* (10), 6763.

Huang, Q., Zasadzinski, J. F., Gray, K. E., Liu, J. Z. & Clause, H. (1989). Electron tunneling study of the normal superconducting states of $Bi_{1.7}Pb_{0.3}Sr_2CaCu_2O_x$. *Physical Review B, 40* (13), 9366 – 9369.

Hussey, N. E., Abdel-Jawad, M., Carrington, A., MacKenzie, A. P., & Balicas, L. (2003). A coherent three-dimensional Fermi surface in a high-transition-temperature superconductor. *Nature, 425* (6960), 814-817.

Jarascan, J. M., et al. (1988). Phys. Rev., **B37**, 9382.

Jeong, G. T., Kye, J. I., Chun, S. H., Lee, S. I., Lee, S., & Khim, Z. G. (1994). Energy gap of thehigh-T_c superconductor $HgBa_2Ca_2Cu_3O_{8+\delta}$ determined by point-contact spectroscopy. *Physical Review B, 49* (21) 15416 – 15419.

Jerome, D., Mazaud, A., Ribault, M., & Bechgaard, K. (1980). Superconductivity in synthetic organic conductor (TMTSF) 2PF6. *Journal de Physique Lettres*, *41* (4), 95-98.

Josephson, B. D., (1962). Possible new effects in superconductive tunneling, *Physics Letters, 1* (7), 251-253.

Jess, P., Hubler, U., Lang, H. P., Guntherodt, H. J., Luders, K., & Antipov, E. V. (1996). Energy gap distribution of $HgBa_2CuO_{4+x}$ investigated by scanning funnelingmicroscopy/spectroscopy. *Journal of Low Temperature Physics,105*, 1243 – 1248.

Kammerlingh, H. O. (1911). *Communications Physics Laboratory University of Leiden*,124C.

Keisuke, M. & Yamamoto, D. (2015). Variational Cluster Approach to S − Wave Pairing in Heavy-Fermion Superconductors, *Physical Review B*,*9* (10), 104508.

Khanna, K. M.,& Kirui, M. S. K. (2002). Anharmonic apical oxygen in high T_c superconductor. *Indian Journal of Pure and Applied Physics,40* (12), 887-895.

Khanna, K. M. (2008). *Superconductivity.* Moi University Press, Eldoret Kenya.

Kim, Y. B., Hempstead, C. F., & Stand, A. R., (1965). Flux-flow resistance in type II-superconductors. *Physical Review, 139* (4A), A1163.

Kivelson, S. A. (2002). Making high T_c higher: A theoretical proposal. *Physica B: Condensed Matter, 318* (1), 61-67.

Kogan, V. G. (1988). Uniaxial superconducting particle in intermediate magnetic fields.*Physical Review B, 38* (10), 7049 – 7050.

Koonce, C. S., Cohen, M. L., Schooley, J. F., Hosler, W. R., & Pfeiffer, E. R. (1967). Superconducting Transition Temperature of Semiconducting SrTiO3. *Physical Review,163*(2), 380.

Kotegawa, H., Ishida, K., Kitaoka, Y.,Muranaka, T., and Akinitsu, J. (2001). *J. Phys. Rev.Lett.*, 87, 127001.

Kotliar, G. (1988). Resonating Valence bonds and d- wave superconductivity. *Physical Review B, 37* (7), 3664 – 3666.

Kresin, V. Z. (1987). On the relation between the energy gap and the critical temperature.*Solid State Communications, 63*(8), 725-727.

Kresin, V. Z., & Wolf, S. A. (1987).Effect of low dimensionality on parameters of high T_c superconductors. *Solid State Communications*, *63*(12),1141-1143.

Kroto, H. W., Heath, J. R., O'Brien, S. C., Curl, R. F., & Smalley, R. E. (1985). C60 buckminsterfullerene. *Nature*,*318* (6042), 162-163.

Krusin-Elbaum L., Greene R. L., Holtzberg, F., Malozemoff A. P., & Yeshurun Y., (1989). Direct measurement of the temperature-dependant magnetic penetration depth in Y-Ba-Cu-O crystals. *Physical review letters*, *62* (2), 217-220.

Kumar, A. S. (2010). High Temperature Superconductors. *Springer Series in Materials Science.*

Laughlin, R. B. (2002). Gossamer superconductivity. *Ar Xiv Preprint Cond-mat/0209269.*

Lawrence, W. E.,& Doniach, S. (1971). In Proc. 12th Int. in *Conf. Low Temp. Phys.* (p.361). Academic Press of Japan, Kyoto.

Lee, P. J. (2001). *Engineering Superconductivity*. Wiley-IEEE Press.

Legget, A. J., (1999). Cuprate superconductivity: dependence of T_c on the c-axis layering structure. *Physical review letters, 83* (2), 392.

Levinsen, J.,& Parish, M. (2015).Strongly interacting two-dimensional Fermi gases. *Annual review of cold atoms and molecules:* Volume 3, 3, 1.

Maeda, H., Tanaka, Y., Fukutomi, M., & Asano, T. (1988). *JPn. JPNJ Appl. Phys.,27*, L209.

Mathias, B. T., Marezio, M., Corenzwit, E., Cooper, A. S., & Barz, H. E. (1972). High-temperature superconductors, the first ternary system. *Science*, *175* (4029), 1465-1466.

Meissner, W., & Ochsenfeld, R. (1933). Ein neuer effekt bei eintritt den supraleitfahigkeit. *Naturwinsseinschaften,21* (44), 787-788.

Maxwell, E. (1950). Isotope effect in the superconductivity of mercury. *Physical Review, 78* (4), 477.

Michael, C., Harvien N., Bosel, M. M., Grandin, A., Deslantes. F., Provast, J., & Raneau, B. (1987). Superconductivity in the Bi-Sr-Cu-O system. *Z. Phys. B, 68,* 421-423.

Mihailovic, D., Foster C. M., Voss, K., & Heegar, A. J. (1990). Application of the polaron-transport theory to δ (ω) in Tl2Ba2Ca1-xGdxCu2O8, YBa2Cu3O7-δ and La2-xSrxCuO4.*Physical Review B, 42,* (13), 7989.

Miyake, K., Schmitt − Rink, S., and Varma, C. M. (1986). Spin-fluctuation-mediated even-parity pairing in heavy-fermion superconductors. *Physical Review B,34* (9), 6554.

Mourachkine, A. (1999). The order parameters for pairing and phase coherence in cuprates. The magnetic origin of the coherent gap. The MCS model of high T_c superconductivity. *Journal of Low Temperature Physics117* (3-4), 401-405.

Mourachkine, A. (2001). Long-range phase coherence and spin fluctuation in Bi2212.*Europhysics Letters, 55,*(Cond-mat/0011080),86.

Mourachkine, A. (2001). Evidence of quasi-ID topological-excitation liquid in Bi2Sr2CaCu2O8+x from tunneling spectroscopy EPL (*Europhysics Letters*)*, 55* (4)*,* 559.

Mourachkine, A. (2001). The distribution of the energy gap and Josephson IcRn products inBi2Sr2O8+x by tunneling spectroscopy. *Journal of Superconductivity, 14* (3)*,* 375-379.

Mourachkine, A. (2001). Quai-ore-dimensional topological-excitation liquid in Bi2Sr2CaCu2O8+x from tunneling spectroscopy. *Superconductor Science and Technology, 14* (6), 329.

Mourachkine, A. (2002). High-Temperature Superconductivity of Cuprates: The nonlinear mechanism and tunneling measurements. (Volume 125). Springer Science and Business Media. *Kluwer Academic Publishers.* Pp13.

Muhlschlegel, B. (1959). Die Thermodynamischen Funktionen des Supraleiters. *Zeitschrift fur Physiks, 155* (3) 313 – 327.

Newns, D.M., Krishnamrthy, H. R., Pattnaik, P. C., Tsuei, C. C., & Kane, C. L. (1992). Saddle-point pairing: An electronic mechanism for superconductivity. *Physical review letters, 69* (8), 1264.

Nagamatsu, J., Nakagawa, N., Muranaka, T.,Zenitani, Y., & Akimitsu, J. (2001). Superconductivity at 39K in magnesium diboride. *Nature,410* (6824), 63-64.

Norman, M. R. (2011).The challenge of unconventional superconductivity.*Science,332* (6062), 196-200.

Onnes, H.K. (1911). The resistance of pure mercury at helium temperatures. *Commun. Phys. Lab. Univ. Leiden, 12* (120), 1.

Ozyuzer, L., Zasadzinski, J. F., Gray, K. E., Liu, J. Z., & Claus, H. (2000). Quasiparticle and Josephson tunneling of overdoped $Bi_2Sr_2CaCu_2O_{8+\delta}$ single crystals. *Phys Rev B* 61:3629 – 3640.

Ozyuzer, L., Zasadzinski, J. F., Kendziora, C., &Gray, K. E.(2000). Quasiparticle and Josephson tunneling of overdoped $Bi_2Sr_2CaCu_2O_{8+\delta}$ single crystals. *Physical ReviewB 61*(5) 3629.

Ozyuzer, L., Yusof, Z., Zasadzinki, J. F., Li, T. W., Hinks, D. G. & Gray, K. E. (1999).Tunneling spectroscopy of $Ti_2Ba_2CuO_6$. *Physica C: superconductivity, 320* (1), 9 – 20.

Parkin, S. S. P., Lee, V. Y., Engler, E. M., Nazzal, A. I., Huang, T. C., Gorman, G. & Beyers, RR. (1988). Bulk superconductivity at 125K in Tl2Ca2Ba2Cu3Ox.*Physical review letters, 60*(24),2539.

Phillips, J. C. (1987). Giant defect-enhanced electron-phonon interaction in ternary copper oxide superconductors. *Physical reviewletters 59* (16), 1856.

Pippard, A. B. (1953). An experimental and theoretical study of the relation between magnetic field and current in a superconductor. *In Proceedings of the Royal Society of London A: Mathematical, Physical and Engineering Sciences.* (Vol. 216, No. 1127 pp. 547-568). The Royal Society.

Poole, C. P., Farach, H. A., and Creswick, R. J. (1995). Superconductivity. *Academic Press,* UK.

Poole, C. P., Horacio, A. and Richard, J. C. (2010). Superconductivity. *Academic*

Press, New York.

Putillin, S. N., & Boyntse, I. (1993). Electron microscopy studies of the mercury based superconductor HgBa2CuO4+δ. *Physica C: Superconductivity, 212* (12),   223-227.

Putillin, S. N., Marezio, M, Antipov, E. V., Capponi, J. J., Chailout, C., Santaro, A., & Tholence, J. L. (1994). Structures and superconductivity in the HgBa2Can-1CunO2n+2+δHomologous series. *In advances in superconductivity VI,*   (pp. 237-242), Springer Japan.

Reynolds, C. A., Serin, W. H., Wright, and Nesbitt, L. B. (1950). *Phys. Rev.,*   *78*, 478.

Rossat-Mignod, J., Regnault, L. P., Vettier, C., Bourges, P., Burlet, P., Bossy, J., Henry,J. Y., & Lapertot, G. (1991). Neutron scattering study of the YBa2Cu3O6+x system. *Physica C: superconductivity, 185,* 86-92.

Satpathy, S. & Martin, R. M. (1987). Electronic structure of the superconducting oxide spirel LiTi2O4.*Physical Review B,36*, 7269.

Scalapino, D. J., Lohnj, E., & Hirsch, J. E. (1986). D-wave pairing near aspin-density-wave instability. *Physical Review,B, 34*(11), 8190.

Schilling, A., Cantoni, M., Guo, J. D., & Ott, H. R. (1993) Superconductivity above130K in the Hg-Ba-Ca-Cu-O System. *Nature*, 363 (6424), 56-58.

Shen, Z-X., Dessau, D. S., Wells, B. O., King, D. M., Spicer, W. E., Arko, A. J., Marshall,D. Lambardo, L. W., Kapitulinik, A., Dickinson, P., Doniach, S., DiCarlo, J.,Loeser, A. G., and Park, C. H. (1993). Anomalously large gap anisotropy in the $a - b$ plane of $Bi_2Sr_2CaCuO_{8+\delta}$. *Physical Review Letters,70* (10) 1553.

Sheng, Z. Z., & Hermann, A. M. (1988). Superconductivity in rare-earth freeTi-Ba-Cu-O System above liquid nitrogen temperature. *Nature*, *332* (6159), $55 - 58$.

Sheng Z. Z., Hermann, A. M., El Ali, A., Almasan C., Estrada, J., Datta, T.,& Matson, R. J. (1988). Superconductivity at 90K in the Ti-Ba-Cu-O System. *Physical reviewletters,60* (10) 937.

Sheng, Z. Z. and Hermann, A. M., (1988). *Nature*, *332*, 55.

Shimada, D., Tsuda N., Paltzer, U., & De Wette, F. W. (1998). The tunneling phonon structures and the calculated phonon density structures and the calculated phonon density of states for Bi2Sr2CaCu2O8.*Physica C: Superconductivity, 298*(3), 195-202.

Sleight, A. W., Gillson, J. L., and Bierstedt, P.E. (1975). *Solid State Commun.,* 17, 23.

Shubnikov, L. V., & Nakhutin, I. E. (1936). Electrical conductivity of a superconducting sphere in the intermediate state. *Nature*.

Stajic, J. (2016). Electrons that Flow like a Fluid. *Science*.

Steglich, F., Arts, J., Bredl, C. D., Lieke, W., Maschede, D., Frauz, W., & Schafer, H. (1979). Superconductivity in the presence of strong Pauli paramagnetism, CeCu2Si2. *Physical Review Letters, 43* (25), 1892.

Sunshine, S. A., et al. (1988). *Phys. Rev.*, *B38*.

Takechi, I., Tsai, J. S., Shimakawa, Y., Manako, T., & Kubo, Y. (1989). Energy Gap of Ti-Ba-Ca-Cu-O compounds by Tunneling. *Physica C: Superconductivity, 158* (1-2), 83 – 87.

Tang, W. H., Ng, C. Y., Yau, C. Y., & Gao, J. (2000). Thickness dependence of superconductivity for YBa2Cu3Oy ultra-thin films. *Superconductor Science and Technology, 13* (5), 580.

Tarascan, J. M., &Bagley, B. G. (1989). Oxygen stoichiometry and the high T_c superconducting oxides.*MRS Bulletin 14* (01), 53-57.

Terashima, W., Ishitaui, Y. W., Che, S. B., & Yoshikawa, A. (2006). Conduction and valence band edge properties hexagonal lnN characteristic by optical measurement. *Physical Static Solid School (C), 3* (6)1850-1853.

Timusk, T., & Statt, B. (1999). The pseudogap in the high-temperature superconductors: an experimental survey, *Report on Progress in Physics 62,* (1)61.

Tsai, J. S., Takeuchi, I., Fujita, J., Miura, S., Terashima, T., Bando, Y., Iijima, K., &Yamamoto, K., (1989). Tunneling study of clean and oriented Y-Ba-Cu-O and Bi-Sr-Ca-Cu-O surfaces. *Physica C: superconductivity, 157*(3), 537 – 550.

Tranquada, J. M., Sternlieb, Axe, J. D., Nakamura, Y., and Uchida, S.(1995). Evidence of stripe correlations of spins and holes in copper oxide superconductors. *Nature*, *375*(6532), 561-563.

Uchida, S. (1997). Spin gap effects on the c-axis and in-plane charge dynamics of high T_c cuprates. *Physica C: Superconductivity, 282*, 12-18.

Vaknin, D., Sinha, S. K., Mancton, D. E., Johnston, D. C., Newsam, J. M., Satinya, C. R., & King Jr, H. E. (1987). Antiferromagnetism in LA2CuO4-y. *Physical review letters, 58* (26), 2802.

Vedeneev, S. I., & Stepanov, V. A. (1994). Superconducting energy gap in single crystals. *Physical Review B, 49*, 9823.

Vladimir Z. Kresin and Stuart A. W. (1990). Fundamentals of Superconductivity Plenum Press

Warren Jr, W. W., Walstedt, R. E., Brennert, G. F., Cava, R. J. Tycko, R., Bell, R. F. & Dabbagh, G. (1989). Cu Spin dynamics and superconducting precursor effects in plates above T_c in YBa2Cu3O6.7. *Physicalreviewletters, 62* (10), 1193.

Wu, M. K., Ashburn, J. R, Torng, C., Hor, P. H., Meng, R. L., Gao, L., Chu, A. (1987). Superconductivity at 93K in new mixed phase Y-Ba-Cu-O compound system at ambient pressure. *Physical Review Letters*, *58* (9), 908.

Wu, T., Mayaffre, H., Krammer, S., Harvatic, M., Berthier, C., Lin, Huang D., Loew, T., Hinkov, V. (2013) Magnetic field enhanced spin freezing on the verge of charge ordering in YBa2Cu3O6-45. *Physical Review B:* 88(1), 014511.

APPENDICES.

Appendix I. Energy Gap to Transition Temperature Ratio for Δ = 20meV.

$\rho=2\Delta/k_B T_c$	T_c (K) for $\Delta = 20$meV
5.000	93.0
5.041	92.8
5.153	90.0
5.270	88.0
5.393	86.0
5.521	84.0
5.656	82.0
5.797	80.0
5.946	78.0
6.102	76.0
6.267	74.0
6.441	72.0
6.625	70.0
6.820	68.0
7.027	66.0
7.246	64.0
7.480	62.0
7.729	60.0
8.000	58.0

Appendix II: Energy Gap to Transition Temperature Ratio for Δ = 62.5meV

$\rho=2\Delta/k_BT_c$	T_c (K) for $\Delta = 62.5\text{meV}$
5.000	289.86
5.103	284.00
5.176	280.00
5.251	276.00
5.328	272.00
5.408	268.00
5.490	264.00
5.574	260.00
5.661	256.00
5.751	252.00
5.844	248.00
5.940	244.00
6.039	240.00
6.141	236.00
6.247	232.00
6.356	228.00
6.470	224.00
6.588	220.00
6.710	216.00
6.836	212.00
6.968	208.00
7.104	204.00
7.246	200.00
7.394	196.00
7.548	192.00
7.709	188.00
7.876	184.00
8.00	181.16

Appendix III: α and Lattice constant a.

$a(\mathring{A})$	$\alpha \times 10^{-12}$ for H=100 G	$\alpha \times 10^{-10}$ for H=10000 G	$\alpha \times 10^{-8}$ for H=500000 G	$\alpha \times 10^{-7}$ For H=3000000 G
1.00	0.833	0.833	0.417	0.250
1.10	1.008	1.008	0.504	0.303
1.20	1.200	1.200	0.610	0.360
1.30	1.408	1.408	0.704	0.423
1.40	1.633	1.633	0.817	0.490
1.50	1.875	1.875	0.938	0.563
1.60	2.133	2.133	1.067	0.640
1.70	2.408	2.408	1.204	0.723
1.80	2.700	2.700	1.350	0.810
1.90	3.008	3.008	1.504	0.903
2.00	3.333	3.333	1.667	1.000
2.10	3.675	3.675	1.838	1.103
2.20	4.033	4.033	2.017	1.210
2.30	4.408	4.408	2.204	1.323
2.40	4.800	4.800	2.400	1.440
2.50	5.208	5.208	2.604	1.563
2.60	5.633	5.633	2.817	1.690
2.70	6.075	6.075	3.038	1.823
2.80	6.533	6.533	3.267	1.96
2,90	7.008	7.008	3.504	2.103
3.00	7.500	7.500	3.750	2.250

Appendix IV: Transition Temperature T_c and Lattice constant a.

$a(\mathring{A})$	T_c (K)
4.56	77.0
4.29	87.0
4.06	97.0
3.87	107.0
3.70	117.0
3.55	127.0
3.42	137.0
3.30	147.0
3.20	157.0
3.10	167.0
3.01	177.0
2.93	187.0
2.85	197.0
2.78	207.0
2.72	217.0
2.66	227.0
2.60	237.0
2.55	247.0
2.50	257.0
2.45	267.0
2.40	277.0
2.36	287.0
2.32	297.0

Appendix V: Magnetic flux and Transition temperature.

T_c(K)	Φ(G/m^2)
77.0	3.10
82.0	3.22
86.8	3.30
91.6	3.38
94.2	3.42
101.4	3.54
108.6	3.65
115.8	3.76
123.0	3.86
130.2	3.96
137.4	4.06
143.0	4.14
154.0	4.28
166.0	4.43
177.0	4.57
188.0	4.70
200.0	4.83
211.0	4.96
223.0	5.08
226.0	5.12
241.0	5.27
256.0	5.42
271.0	5.57
286.0	5.71
300.0	5.84